The influence of the polar head-group of synthetic cationic lipids on the transfection efficiency mediated by niosomes in rat retina and brain

E. Ojeda[a, b], G. Puras[a, b], M. Agirre[a, b], J. Zarate[a, b], S. Grijalvo[b, c], R. Eritja[b, c],
G. Martinez-Navarrete[b, d], C. Soto-Sánchez[b, d], A. Diaz-Tahoces[b, d], M. Aviles-Trigueros[e],
E. Fernández[b, d], J.L. Pedraz[a, b,*]

[a]NanoBioCel Group, University of Basque Country (UPV/EHU), Vitoria-Gasteiz, Spain
[b]Biomedical Research Networking Center in Bioengineering, Biomaterials and Nanomedicine (CIBER-BBN), Vitoria-Gasteiz, Spain
[c]Institute of Advanced Chemistry of Catalonia, IQAC-CSIC, Barcelona, Spain
[d]Neuroprothesis and Neuroengineering Research Group, Miguel Hernández University, Spain
[e]Laboratory of Experimental Ophthalmology, Faculty of Medicine, University of Murcia, Regional Campus of International Excellence "Campus Mare Nostrum", Murcia, Spain.

Abstract.
The development of novel non-viral delivery vehicles is essential in the search of more efficient strategies for retina and brain diseases. Herein, optimized niosome formulations prepared by oil-in water (o/w) and film-hydration techniques were characterized in terms of size, PDI, zeta potential, morphology and stability. Three ionizable glycerol-based cationic lipids containing a primary amine group (lipid **1**), a triglycine group (lipid **2**) and a dimethylamino ethyl pendent group (lipid **3**) as polar head-groups were part of such niosomes. Upon the addition of pCMS-EGFP plasmid, nioplexes were obtained at different cationic lipid/DNA ratios (w/w). The resultant nioplexes were further physicochemically characterized and evaluated to condense, release and protect the DNA against enzymatic digestion. In vitro experiments were performed to evaluate transfection efficiency and cell viability in HEK-293, ARPE-19 and PECC cells. Interestingly, niosome formulations based on lipid **3** showed better transfection efficiencies in ARPE-19 and PECC cells than the rest of cationic lipids showed in this study. In vivo experiments in rat retina after intravitreal and subretinal injections together with in rat brain after cerebral cortex administration showed promising transfection efficiencies when niosome formulations based on lipid **3** were used. These results provide new insights for the development of non-viral vectors based on cationic lipids and their applications for efficient delivery of genetic material to the retina and brain.

Keywords. Niosomes; Gene delivery; Non-viral vector; Cationic lipid; Retina; Brain

INTRODUCTION

Gene therapy is a challenging field that is emerging as a promising strategy for the treatment of several diseases [1]. Concretely, non-viral vectors have attracted the interest of the scientific community because, compared to viral vectors, they offer a safer way to deliver genetic material, as they do not exhibit antigen-specific immune and inflammatory response, are cheaper, easy to elaborate and the size of DNA inserted is theoretically unlimited [2]. Nevertheless, their low transfection efficiencies and the transient gene expression are the main concerns that these carriers have to overcome to reach clinical practice. There is a wide range of non-viral vectors described in the literature, such as those composed of polymers, lipids or peptides [3-5]. Among lipidic systems, liposomes are the most common vectors. However, our research group has previously described that niosomes are a promising alternative to liposomes for gene delivery purposes. Niosomes are carrier systems that form vesicles with a bilayer structure and compared to liposomes they are recognized for their low cost and superior chemical and storage stabilities. Nevertheless, few reports have been focused on their application for gene delivery purposes [6,7].

Unlike liposomes, which are elaborated with phospholipids, niosomes for gene delivery purposes are typically based on nonionic surfactants to form more stable emulsions. In addition, helper lipids are also added to the formulations to enhance the physicochemical properties of the emulsion and finally, the cationic lipids, whose structural and physical properties clearly influence the transfection efficiency and toxicity [8-10].

Cationic lipids for gene delivery purposes usually contain four functional domains (hydrophobic group, linker group, hydrophilic head-group and backbone), which affect some important physicochemical parameters, such as the flexibility, stability, biodegradability, the level of hydration, interaction with DNA and its condensation [11-14]. In our previous work [15] the influence of the polar head-group on transfection efficiency together with cell viability was studied in HEK-293, ARPE-19 and MSC-D1 cells. Although promising results were obtained, such studies were performed with lipids containing a serinol backbone, which due to its low biodegradability reduced significantly cell viability. Therefore in the present manuscript, we have modified the serinol backbone by a glycerol one in order to improve the design of the niosomes formulation for in vivo retinal and brain delivery purposes.

Regarding the applications of gene therapy, the eye has favorable characteristics for this type of therapy, such as small size, immune-privileged position and well-defined compartmentalized anatomy, which minimize potential adverse reactions [16]. Additionally, most of the devastating inherent diseases in the eye are well described and their genetic background is also well known. However, at present few effective treatments are available for inherent retinal diseases. Therefore, research on the design of novel formulations for gene delivery to the retina represents a promising approach in order to translate animal research into clinical trials [17]. On the other hand, neurological disorders are the most difficult diseases to treat with clinical pharmacological approaches, mainly due to the complexity of the nervous system and the different brain physical barriers that drugs need to overcome after systemic administration [18]. Gene therapy represents a promising alternative to the traditional pharmacological approaches to face many devastating genetic diseases of the brain, such as Batten disease [19], Canavan disease [20] or Parkinson's disease [21]. In the past few years many gene transfer methods have been developed to treat retinal and brain diseases. However, all gene clinical trials are based on viral vectors that generate moderate optimism to drive the field forward. Therefore, we present an alternative and a safer approach to confront inherent retinal and brain disorders by the use of niosomes as non-viral carriers for gene delivery purposes.

Consequently, in the present study, we designed niosomes vectors for retinal and brain delivery purposes based on three synthetic ionizable cationic lipids containing polysorbate 80, as a non-ionic surfactant and squalene, as a helper lipid. These cationic lipids

had three different functional domains: 1) an hydrophobic tail formed by two saturated hydrocarbonated alkyl chains of fourteen atoms of carbons in length; 2) a polar head formed by an amino group (lipid **1**), a glycine triglycine (lipid **2**) and a dimethylaminoethyl group (lipid **3**) and 3) a glycerol-based building block. Niosomes prepared by the oil-in-water emulsion (o/w) and film hydration techniques were characterized in terms of size, PDI, zeta potential, morphology and physical stability. Upon the addition of the pCMS-EGFP reporter plasmid, we obtained nioplexes at different cationic lipid/DNA ratios (w/w). The influence of cationic lipid/DNA ratios on particle size, zeta potential and the ability to condense, release and protect DNA from enzymatic digestion was analyzed. In vitro experiments were performed and analyzed by flow cytometry to evaluate the most promising formulations in terms of transfection efficiency, viability and mean fluorescence intensity (MFI) in human embryonic kidney 293 cells (HEK-293), retinal pigment epithelia 19 cells (ARPE-19) and rat primary embryonic cerebral cortex cells (PECC). In order to move forward and according to the previous characterization results of the noisome formulations and nioplexes, we carried out some preliminary in vivo studies by confocal microscopy to evaluate transfection efficiency of the most promising formulation in the rat retina after intravitreal and subretinal injection and in the rat brain after injection in the cerebral cortex.

2. Material and methods

2.1. Material

All reactions were carried out under an inert atmosphere of argon. Flash column chromatography was carried out on silica gel SDS 0.063e0.2 mm/70e230 mesh. ^{1}H and ^{13}C NMR spectra were recorded at 25 ºC on a Varian Mercury 400 MHz spectrometer using deuterated solvents. Tetramethylsilane (TMS) was used as an internal reference (0 ppm) for ^{1}H spectra recorded in CDCl$_3$ and the residual signal of the solvent (77.1 ppm) for ^{13}C spectra. For CD$_3$OD and d$_6$-DMSO the residual signal of the solvent was used as a reference. Chemical shifts are reported in parts per million (ppm), coupling constants (J) in Hz and multiplicity as follows: s (singlet), d (doublet), t (triplet), q (quadruplet), quint (quintuplet), m (multiplet) and br (broad signal). Electrospray ionization mass spectra (ESI-MS) were recorded on a Micromass ZQ instrument with a single quadrupole detector coupled to an HPLC, and high resolution (HR) ESI-MS on an Agilent 1100 LC/MS-TOF instrument (Servei d'Espectrometría de Masses, Universitat de Barcelona). HEK-293 cells, ARPE-19 cells, Eagle's Minimal Essential medium with Earle's BSS and 2 mM L-glutamine (EMEM) were obtained from the American Type Culture Collection (ATCC). Dulbecco's Modified Eagle's medium Han's Nutrient Mixture F-12 (1:1), Trypsine, Hank's Balanced Salt Solution (HBSS), Neurobasal medium (NB), Fetal bovine Serum (FBS), B27® and Glutamax™ supplements and Penicillin-Streptomycin (Pen/Strep) antibiotics were purchased from Gibco® (San Diego, California, US). The plasmid pCMS-EGFP was purchased from Plasmid Factory (Bielefeld, Germany). The gel electrophoresis materials and gel red solution were acquired from Bio-Rad (Madrid, Spain). DNase I, sodium dodecyl sulfate (SDS), squalene, polysorbate 80, PBS and paraformaldehyde were purchased from SigmaeAldrich (Madrid, Spain), and dichloromethane (DCM) was purchased from Panreac (Barcelona, Spain). Opti-MEM® reduced medium, antibiotic/antimycotic solution and Lipofectmanine™ 2000 transfection reagent were acquired from Invitrogen (San Diego, California, US). The BD Viaprobe kit was obtained from BD Biosciences (Belgium).

2.2. Synthesis of ionizable cationic amino lipids

The synthesis of the ionizable cationic amino lipids is summarized in Supplementary Data Scheme S1. Synthesis of tert-butyl-N-[2-[[2-[[2-[2,3-di(tetradecoxy)propylamino]-2-oxo-ethyl]amino]- 2-oxo-ethyl]-amino]-2-oxo-ethyl]carbamate (**3**). Firstly, the carboxylic acid activation was carried out as follows: glycine tripeptide (2.0 eq) and N-hydroxysuccinimide (2.1

eq) were dissolved in DCM (3 mL) and the solution was stirred for a couple of minutes. Then, EDC (2.2 eq) was added. The reaction was stirred overnight at room temperature. The organic layer was washed with water (3 x 5 mL) and dried over anhydrous MgSO$_4$. The combined organic layers were reduced in vacuo and the anticipated crude was used in the next step without further purification. Cationic lipid **1** (compound 2) (100 mg; 0.206 mmol) was added over the activated tripeptide. Reaction was heated at 60 ºC and stirred overnight. The solvent was evaporated and the resultant crude was purified by flash chromatography (DCM/MeOH 5%).

Synthesis of 2-[[2-[(2-aminoacetyl)amino]acetyl]amino]-N-[2,3-di(tetradecoxy)propyl]-acetamide (**4**, lipid **2**). Boc-protected alkyl tripeptide 3 (50 mg; 0.066 mmol) was dissolved in DCM (1 mL) and trifluoroacetic acid was subsequently added (10%). The solution was stirred for one at room temperature. The solvent was removed until dryness. Finally, the anticipated trifluoroacetate salt was dissolved in a mixture of AcOEt:MeOH (3:2) and carbonate on polymer support (20 eq) was added. The mixture was stirred for 1 h at room temperature. The resin was filtered off and solvent was reduced until dryness obtaining the corresponding cationic lipid **4**, which was used without further purification.

Synthesis of 1-(2-dimethylaminoethyl)-3-[2,3-di(tetradecoxy) propyl]urea (**5**, lipid **3**). Previously, p-nitrophenyl-chloroformate (2.5 eq) and amino diol 2 (100 mg; 0.206 mmol) were dissolved in a mixture of tetrahydrofurane and DCM (1:1) (6 mL). The reaction was cooled at 0ºC and DIEA (2.5 eq) was carefully added dropwise. The solution was stirred for 4 h and heated at room temperature. The solvent was removed and the resultant crude was used in the next step without further purification. The yellow crude was dissolved in DMF (3 mL) and the corresponding dimethylamine derivative (1.1 eq) was added dropwise. The reaction was stirred overnight at room temperature. Finally, solvent was removed and the resultant crude was purified by flash chromatography (DCM:MeOH 5%e10%).

2.3. Preparation of niosomes and nioplexes

Niosomes based on three different synthetic cationic lipids were prepared using the o/w emulsification and the film-hydration techniques, as previously reported [15]. In the o/w emulsification technique, the cationic lipid (5 mg) was gently grounded with 23 ml of squalene and then emulsified in an aqueous phase containing polysorbate 80 (0.5%, w/w). The emulsion was obtained by sonication (Branson Sonifier 250, Danbury) for 30 s at 50W. The organic solvent was removed from the emulsion by evaporation under magnetic agitation for 3 h. In the film-hydration technique, the lipid compounds (5 mg cationic lipid and 23 ml squalene) were grounded in DCM, and then the solvent was evaporated under magnetic agitation for 3 h. Then, the lipid film was hydrated with the aqueous phase containing the non-ionic surfactant polysorbate 80 (0.5%, w/ w), and the emulsion was obtained by sonication for 30 s at 50 W. The final cationic lipid concentration was 1 mg/ml.

The nioplexes (niosome/DNA vectors) were elaborated by mixing an appropriate volume of a stock solution of the pCMS-EGFP plasmid (0.5 mg/ml), which was propagated and purified as previously reported [15] with different volumes of the niosome suspensions for 30 min at room temperature. The niosome/DNA ratio was referred as the ratio of cationic lipid to DNA (w/w). The stock solutions of cationic lipids (1 mg/ml) correspond to the following molar concentrations: 2.07 mM (Lipid **1**, MW 484), 1.53 mM (Lipid **2**, MW 654), and 1.67 mM (Lipid **3**, MW 598). The stock solution of plasmid pCMS-EGFP (0.5 mg/ml) was estimated to be around 0.137 mM (pCMS-EGFP, 5541 bp, average MW 3657060).

2.4. Size and zeta potential of niosomes and nioplexes and Cryo- TEM analysis of niosomes

Dynamic Light Scattering (DLS) and Laser Doppler Velocimetry (LDV) were applied to measure hydrodymanic diameter and zeta potential of the niosomes and nioplexes in a

Zetasizer Nano ZS (Malvern Instrument, UK). Particle size reported as hydrodynamic diameter was obtained by Z-average (cumulants means). Niosomes or nioplexes were resuspended 0.1 mM NaCl solution. All measurements were carried out in triplicate. Only data that met the quality criteria according to the software program were included in the study. Cryo Transmission Electron Microscopy (Cryo-TEM) was employed to analyze the morphology of niosomes, as previously described [15].

2.5. Physical stability study of niosomes

Niosomes based on three different synthetic cationic lipids were storage for 100 days at 4 ºC and 25 ºC. Their physical stability was determined by monitoring the particle size and zeta potential during storage time. All samples were measured in triplicate.

2.6. Agarose gel electrophoresis studies of nioplexes

In order to analyze the ability of the niosomes to condensate, release and protect the DNA, we carried out an agarose gel electrophoresis assay with the nioplexes at different cationic lipid/DNA ratios (200 ng of DNA per well). The agarose gel (0.8%) was immersed in a Tris-acetate-EDTA buffer and exposed for 30 min to 120 V. DNA bands were stained with GelRed™ (Biotium, Hayward, California, USA) and images were observed with a ChemiDoc™ MP Imaging System. SDS 3.5% solution and DNase I enzyme (1 U DNase I per 2.5 mg DNA) were added to the samples to evaluate the release and protection, respectively. The integrity of the DNA in each sample was compared to a control of untreated DNA.

2.7. Cell culture and in vitro transfection protocols

HEK-293 and ARPE-19 cells were seeded in 24 well plates at an initial density of 15 x 10^4 and 10 x 10^4 cell per well, with 300 µl of EMEM containing 10% horse serum and 300 µl of D-MEM/F-12 containing 10% bovine serum, respectively. Cells were incubated overnight to achieve 70-90% of confluence at the time of transfection. Experimental procedures for PECC cells were carried out conformed to the directive 2010/63/EU of the European Parliament and of the Council, and the RD 53/2013 Spanish regulation on the protection of animals use for scientific purposes and was approved by the Miguel Hernandez University Committee for Animal use in Laboratory. Dissociated cultures of hippocampal neurons were obtained from E17.5 rat embryos (Sprague Dawley) and preserved in HBSS during extraction. Then, trypsin was added to the medium and incubated in a bath at 37 ºC for chemical dissociation. Subsequently, the tissue was mechanically dissociated in NB/FBS and the cell density was determined using a hemocytometer. Cells were seeded on glass coverslips (Thermo Scientific) at approximately 100,000 cells/well cell density in a 12 well plate (Corning Incorporated) and maintained in a NB/FBS medium supplemented with B27, Glutamax and Pen/Strep (1:100 dilution) in an incubator at 37 ºC and 5% CO_2. At the time of transfection assay, the regular growth mediums were removed from ARPE-19, HEK-293 and PECC cells, and the cells were exposed to nioplexes resuspended in Opti- MEM® transfection medium at different cationic lipid/DNA ratios. The amount of plasmid for each well was 1.25 µg. Each formulation was used in triplicate. After 4 h of incubation at 37 ºC, the nioplexes were replaced by 300 µl of regular growth medium. Cells were allowed to grow for 72 h until flow cytometry analysis. Following the manufacturer's protocol, Lipofectamine™ 2000 was used in combination with pDNA as a transfection positive control.

2.8. Transfection efficiency and cell viability

Flow cytometry analysis was conducted using a FACSCalibur system flow cytometer (Becton Dickinson Bioscience, San Jose, USA) in order to quantify the percentage of EGFP positive cells. Cells were washed twice with PBS and detached from the microplate with 200 µl of trypsin/EDTA. Once the cells were detached, 400 µl of their respective normal growth

medium were added and directly introduced into the flow cytometer. Transfection efficiency was expressed as the percentage of EGFP positive cells at 525 nm (FL1) after excluding dead cells. MFI data were obtained from live positive cells at 525 nm (FL1). Cell viability of the cells was evaluated using 5 µL of BD Via Probe reagent in each sample and positive cells were excluded from the EGFP expression analysis. The fluorescent signal corresponding to dead cells was measured at 650 nm (FL3). Control samples (non-transfected cells) were displayed on a forward scatter (FSC) versus side scatter (SSC) dot plot to establish a collection gate and exclude cells debris. Control samples containing Lipofectamine™ 2000 transfected cells without BD-Via Probe, and non-transfected cells with BD-Via Probe were used to compensate FL2 signal in FL1 and FL3 channels. For each sample 10,000 events were collected. Each formulation was analyzed in triplicate.

2.9. In vivo studies in rats

Adult male Sprague Dawley rats (6-7 weeks old, 200-300 g weight) were used as experimental animals. All experimental procedures were carried out in accordance with the Spanish and European Union regulations for the use of animals in research and the Association for Research in Vision and Ophthalmology (ARVO) statement for the use of animals in ophthalmic and vision research and supervised by the Miguel Hernandez University Standing Committee for Animal Use in Laboratory. The surgical procedures used for the administration of the vectors in the retina and brain have been described elsewhere [22,23].

2.9.1. Intravitreal and subretinal injections

Six adult male Sprague Dawley rats were used for this assay; three rats received injection of nioplexes by intravitreal and three by subretinal route. Injections were performed under an operating microscope (Zeiss OPMI® pico; Carl Zeiss Meditec GmbH, Jena, Germany) with the aid of a Hamilton microsyringe (Hamilton Co., Reno, NV). A bent 34-gage needle was used to inject into the vitreous of the left eye, closely adjacent to the ora serrata without touching the lens. In order to deliver the formulation into the subretinal space, the needle was passed through the sclerotomy 2 mm posterior to ora serrata and in a tangential direction toward the posterior retinal pole along the subretinal space. Successful administration was confirmed by the appearance of a partial retinal detachment by direct ophthalmoscopy of the eye fundus. The untreated right eye, served as a control. Seven days post-injection, the rats were sacrificed and perfused with saline solution (0.9%) followed by paraformaldehyde (4%) in phosphate buffer (0.1M, pH 7.2-7.4) at 4 ºC.

2.9.2. Evaluation of EGFP expression in rat retinas

All preparations were mounted as follows. Both eyes from each group were enucleated and immersed for 1 h in a solution of PBS with paraformaldehyde (4%). Later, the retinas were dissected as whole-mounts by making four radial cuts. Retinal orientation was maintained by making the deepest radial cut in the superior retina. The retinas were post-fixed for 1 h in the same fixative medium, rinsed with PBS, and mounted in poly-L-lysine coated microscope slides with the vitreal side facing up, covered with anti-fading mounting media containing glycerol (50%) and *p*-phenylenediamine (0.04%) in sodium carbonate buffer (0.1 M, pH 9.0). In order to identify retinal nuclei, the samples were stained with Hoechst 33342. 5 mg/ml of dye was added to the samples and left for 5 min, then samples were thoroughly washed with PBS (0.1 M) and covered with anti-fading mounting media. EGFP expression and Hoechst 33342 staining were evaluated with a Leica TCS SPE spectral confocal microscope (Leica Microsystems GmbH, Wetzlar, Germany). Images were processed, montaged and composed digitally using ImageJ, (National Institutes of Health, Bethesda, MD) and Adobe® Photoshop® CS5.1 (Adobe Systems Inc, San Jose, CA) software. Hoechst 33342 staining was pseudocolored in red for better contrast.

2.9.3. Brain administration

Data were obtained from male Spraguee Dawley adult rats. Surgical analgesia was induced by buprenorphine (0.025 mg/kg, s.c) and anesthesia and sedation were induced by a cocktail of ketamine HCl (40 mg/kg, i.p) and diazepam (5 mg/kg, i.p). Subsequently, the anesthesia was continued and maintained with a mix of oxygen and 2% of isofluorane for the rest of the surgery. The effect of the anesthesia was continuously evaluated by monitoring heart rate, blinking and toe pinch reflexes. Rats were pre-treated with dexamethasone (1 mg/kg, i.p) 24 h previous to the surgery and administered again 20 min before and 24 h after surgery. Briefly, we drilled a small craniotomy while 0.8 µl of nioplexes were incubated for 30 min at room temperature. Then, the nioplexes were injected inside the cerebral cortex with a microsyringe (Hamilton company, 33-gage needle) 1 mm. Once the procedure was finished, the animals were housed in their own cages for 3 days. A post-surgery treatment with antibiotics (enroflorxacine 25 mg/kg, s.c), anti-inflammatory and analgesic drugs (meloxicam 2 mg/kg, s.c) was administrated.

2.9.4. Evaluation of EGFP expression in the rat brain

Intracardiac perfusion with phosphate buffer solution followed by paraformaldehyde (4%) was performed for an initial fixation. Then, the brains were preserved in paraformaldehyde (4%) and cryoprotected in sucrose solution (30%) with PBS before slicing. A cryostat (HM 550; Microm International GmbH, Walldorf, Germany) was used to obtain slices of 20 mm from coronal frozen sections adjacent to the injection area. Once the slices were mounted for immunohistochemistry processing, sections were incubated in normal bovine serum (10%) (Jackson, West Grove, PA, USA) with Triton X-100 (0.5%) for blocking of non-specific staining. Then, the samples were incubated overnight at room temperature with chicken anti-GFP (Invotrogen, 1:100) and rabbit anti-NeuN (Millipore, 1:300) antibodies diluted in PBS containing Triton- X100 (0.5%). Later, sections were washed in PBS and incubated for 1 h with Alexa Fluor 488-conjugated donkey anti-rabbit IgG and Alexa fluor 555-conjugated donkey anti-chicken IgG (Invitrogen, 1:100). Hoechst 33342 was used to label the cell nuclei. Finally, sections were mounted for imaging and analyzed with a Leica TCS SPE fluorescence microscope (Leica, Microsystems GmbH, Germany). Hoechst 33342 staining was pseudocolored in red for better contrast.

3. Results and discussion

3.1. Synthesis of ionizable cationic amino lipids

The search of pH-responsive drug delivery systems is one of the main strategies that have been used to carry out more efficient processes of drug release in acid environment. This mechanism normally protects therapeutic molecules at physiological pH whereas accelerates such release in the presence of acid pH caused by late endosomes or lysosomes in which pH can vary from 6.5 to 4.5, respectively. This pH dependence on mediating cellular internalization has been recently reported for eliciting gene silencing in vivo [24].

In this systematic study, a tight correlation between acid dissociation constant (pKa) value and activity of cationic lipid based combinatorial libraries was determined by optimizing several variables like lipid-chain unsaturation, linker chemistry and polar head nature. Interestingly, an optimum pKa (6.2-6.5) was established as an ideal value in order to design new liposomal drug delivery systems [24]. Specifically, this optimal relationship between pKa and silencing activity was successfully found for amino lipid derivatives containing dimethylaminoethyl as a cationic pendent group. This correlation in the transfection activity was also observed in our recent work based on serinol amino lipid derivatives [15]. These findings made us to consider the possibility of introducing this potential modification in our glycerol-based cationic lipid **1** (Fig. 1) which efficiently promoted cellular uptake with improved

values compared to commercially available cationic lipids. As comparison purposes, we also selected triglycine tripeptide in its free amine form in order to investigate further additional effects that could govern transfection efficiency processes when increased the polarpendent group electronic nature.

The synthetic strategy for obtaining our small library of glycerolbased cationic lipids is displayed in scheme S1 (see supplementary part for additional details). The synthesis of the cationic lipid **1** (compound **2**) was previously reported by our research group [7]. In order to further functionalize the free amine group of the amino lipid 2 with a triglycine peptide, carboxylic acid activation with 1-ethyl-3-(3-dimethylaminopropyl)carbodiimide (EDC) and NHydroxysuccinimide (NHS) was carried out by using standard activation protocols. Thus, the anticipated Boc-protectedtripeptide- amino lipid **3** was obtained with moderate yields after purifying by flash chromatography (70%). Final Boc-deprotection was efficiently done with acid treatment (10% trifluoroacetic acid) in DCM, which afforded the corresponding free amine in its trifluoroacetate form. Treatment with carbonate polymer support liberated the amine and the expected triglycine-amino lipid derivative **4** (cationic lipid **2**) was obtained after resin filtration (87%). Finally, the introduction of the dimethylaminoethyl pendent group was accomplished by activating the amine group from amino lipid **2** with p-nitrophenyl-chloroformate according to well-stablished protocols [15]. Final nucleophilic reaction introduced the corresponding dimethylaminoethyl residue and generated the expected urea derivative **5** (cationic lipid **3**) with moderate yield (65%). Since these modifications have not been studied yet, we tentatively chose these three pendant groups in order to be incorporated to the glycerol building block (lipid **1**, lipid **2** and lipid **3**).
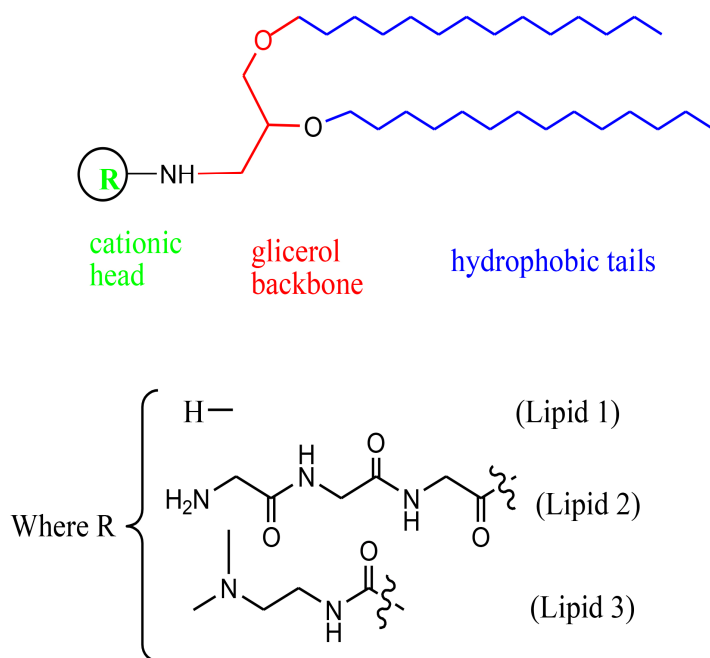

Fig. 1. Chemical structures of cationic lipids. Lipid **1**: 2, 3-bis (tetradecyloxy) propan-1- amine. Lipid **2**: 2-amino-N-(((((2, 3-bis (tetradecyloxy) propyl) carbamoyl) methyl) carbamoyl) methyl) acetamide. Lipid **3**: 1-(2-dimethylaminoethyl)-3-[2,3-di (tetradecoxy) propyl] urea.

3.2. Particle size, PDI, zeta potential and morphology of niosomes

Niosomes based on the three cationic lipids prepared by o/w emulsion and film-hydration techniques were characterized in terms of Z-average (cumulants) size, PDI, zeta potential and

morphology (Fig. 2). We observed that zeta potential values were similar in both techniques for the niosome formulations based on lipid **1** (+47 mV) and lipid **3** (+43 and + 36 mV for o/w emulsion and film hydration, respectively) (Fig. 2A lines). On the other hand, for the niosomes prepared with the lipid **2**, there was a considerable difference of 20 mV in the zeta potential between the two techniques (+37 and + 59 mV for o/w emulsion and film-hydration, respectively) (Fig. 2A, lines). In any case, all niosome formulations exhibited positive zeta values over 30 mV, which enhanced the formation of stable suspensions due to the repulsion among the positively charged particles [25]. Additionally, these positive charges also allowed an easy interaction with the negatively charged cell surfaces to increase cell uptake [26].

	Pdi Values			
	o/w emulsion		FilmHydration	
Niosomes	*PDI*	*SD*	*PDI*	*SD*
Lipid 1	0.197	0.007	0.358	0.009
Lipid 2	0.176	0.02	0.996	0.006
Lipid 3	0.216	0.011	0.561	0.104
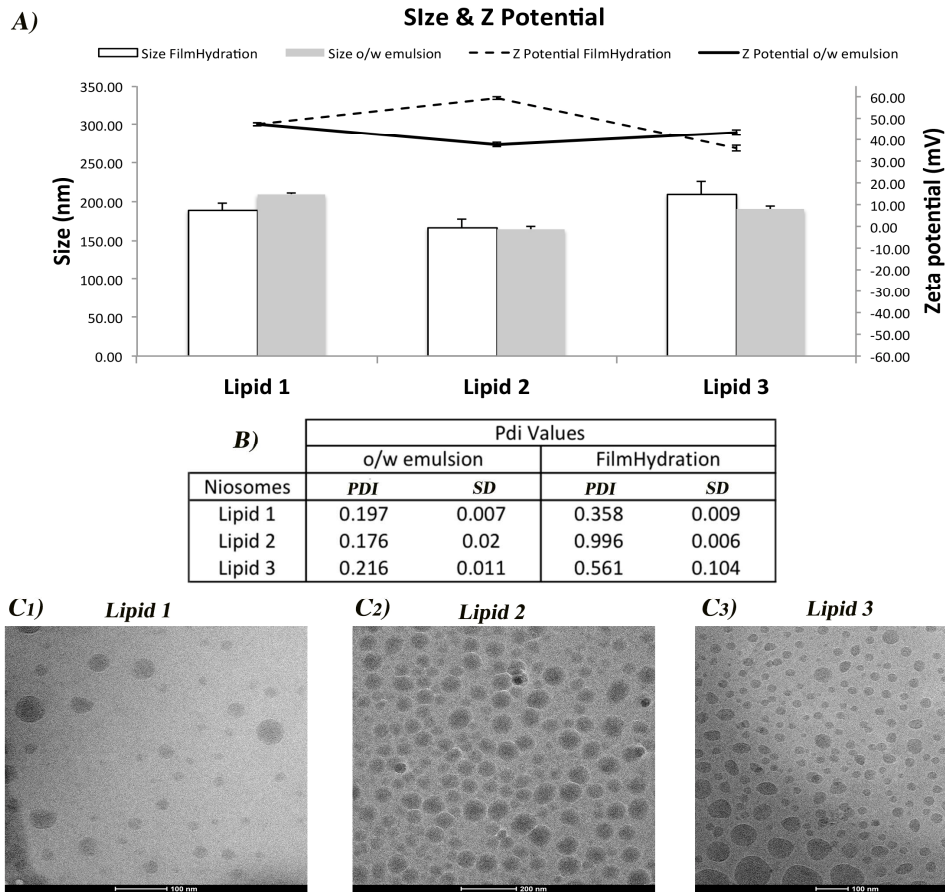
Fig. 2. Physicochemical characterization of niosomes based on lipid **1**, **2** and **3**. A) Z-average (cumulants) size (white and gray bars, which correspond to niosomes prepared by filmhydration and o/w emulsion techniques, respectively) and zeta potential values (dotted and continuous lines which correspond to niosomes prepared by film-hydration and o/w emulsion techniques, respectively). B) PDI values. Each value represents the mean ± standard deviation of three measurements. C) Cryo-TEM images of niosomes prepared by the o/ w emulsion technique. C1) Niosomes based on lipid **1**, C2) niosomes based on lipid **2** and C3) niosomes based on lipid **3**. Scale bar for figures C1 and C3 = 100 nm and for figure C2 = 200 nm.

Regarding particle size values (Fig. 2A, bars), we did not find remarkable differences between the niosomes when they were elaborated by the o/w emulsion or film-hydration technique. In all cases, the particle size was around 200 nm. As a homogeneity parameter of the suspensions, we determined the polydispersity index (PDI) (Fig. 2B). Lower PDI values

(0.19, 0.17 and 0.21 for lipid **1**, **2** and **3**, respectively) were found in niosomes prepared by o/w emulsion when they were compared to niosomes prepared by film hydration technique (0.35, 0.99 and 0.51 for lipid **1**, **2** and **3**, respectively), which showed that the size distribution of niosomes prepared by the o/w emulsion was narrower than the size distribution obtained by film-hydration technique. Since it has been previously reported that narrow distribution of the PDI values enhances the uptake and posterior internalization process of the nanoparticles [27,28], we decided to discard the niosomes prepared by the film-hydration technique for the following experiments.

The morphology of niosomes based on the three cationic lipids and elaborated by the o/w emulsion technique was analyzed by Cryo-TEM (Fig. 2C1, C2 and C3). We observed that all niosomes adopted a spherical and homogeneous morphology. Additionally, the size observed in all niosome formulations by Cryo-TEM (around 100 nm) appeared to be smaller than the sizes reported by dynamic light scattering (around 200 nm, Fig. 2A, bars). Differences in the reported size between DLS and Cryo-TEM techniques could be explained by the treatment of the sample when are processed by both analyses [15].

Based on the data obtained from the physicochemical properties of the niosome formulations, such as size (around 200 nm, Fig. 2A bars), zeta potential (over +37 mV, Fig. 2A lines), morphology (spherical and homogeneous, Fig. 2C 1,2,3) and the significant differences in the PDI values (Fig. 2B), we determined that the niosomes prepared by o/w emulsion technique were the most suitable candidates for the following assays.

3.3. Physical stability of niosomes

Physical stability of niosomes based on the three cationic lipids prepared by o/w emulsion technique is represented on Fig. 3, as a measure of particle size and zeta potential value over the time at 4 and 25 ºC. Regarding zeta potential data, all the niosomes stored at 4 ºC did not show relevant changes (Fig. 3A, B and C lines), especially niosomes based on lipid 2 (þ40 mV, Fig. 3B continued line). On the other hand, when formulations were stored at 25 ºC, remarkable decreases on the zeta potential values were found on niosomes elaborated with lipid 1 and 3 from +40 to -20 mV (Fig. 3A dot line) and from +43 to +2 mV (Fig. 3C dot line), respectively. This decrease at temperatures around 25 ºC can be explained by the re-orientation of crystalline structure of the lipids at high temperatures that is followed by a change on the particle surface, which reduces the zeta potential [29]. The size of the niosomes, as shown in Fig. 3 (gray bars), remained stable for all conditions at 4 ºC. However at 25 ºC storage temperature, niosomes based on lipid 3 increased their size (250 nm) after 100 days (Fig. 3C, white bars). This increase of the particle size can be caused by gradual diminution of the positive charges of the particles that decreases electrostatic repulsion and generates aggregates [25].

In general, more stable formulations over the time in terms of size and charge were achieved at 4 ºC, where the positive superficial charge of niosomes last longer time. At this temperature condition, the high charges avoid the formation of niosome aggregates due to electrostatic repulsion forces. These findings about the zeta potential and size of the niosomes suggest that storage temperature plays an important role in the stability of our niosomes. Moreover, these data also highlighted the participation of the polar head-groups in the physical stability of niosomes, where the implication is more evident in the zeta potential values at 25 ºC. Similar results were observed in previous reported data [15].
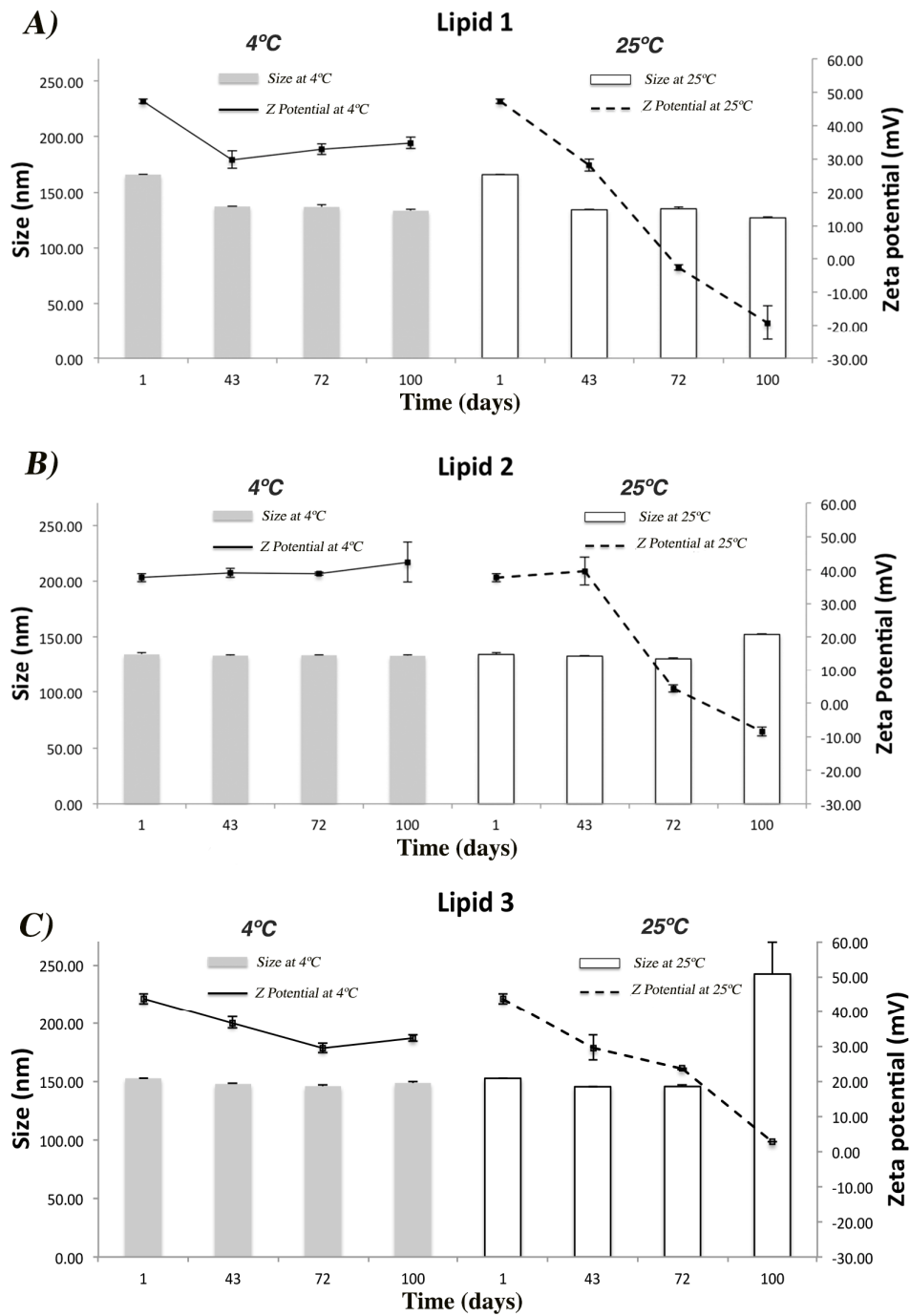
Fig. 3. Physical stability of niosomes based on lipid 1 (A), lipid 2 (B) and lipid 3 (C) following storage at 4 ºC and 25 ºC for 100 days. Gray and white bars correspond to Z-average (cumulants) size obtained at 4 ºC and 25 ºC, respectively, while continuous and dotted lines correspond to zeta values obtained at 4 ºC and 25 ºC. Each value represents the mean ± standard deviation (SD) from three independent experiments.
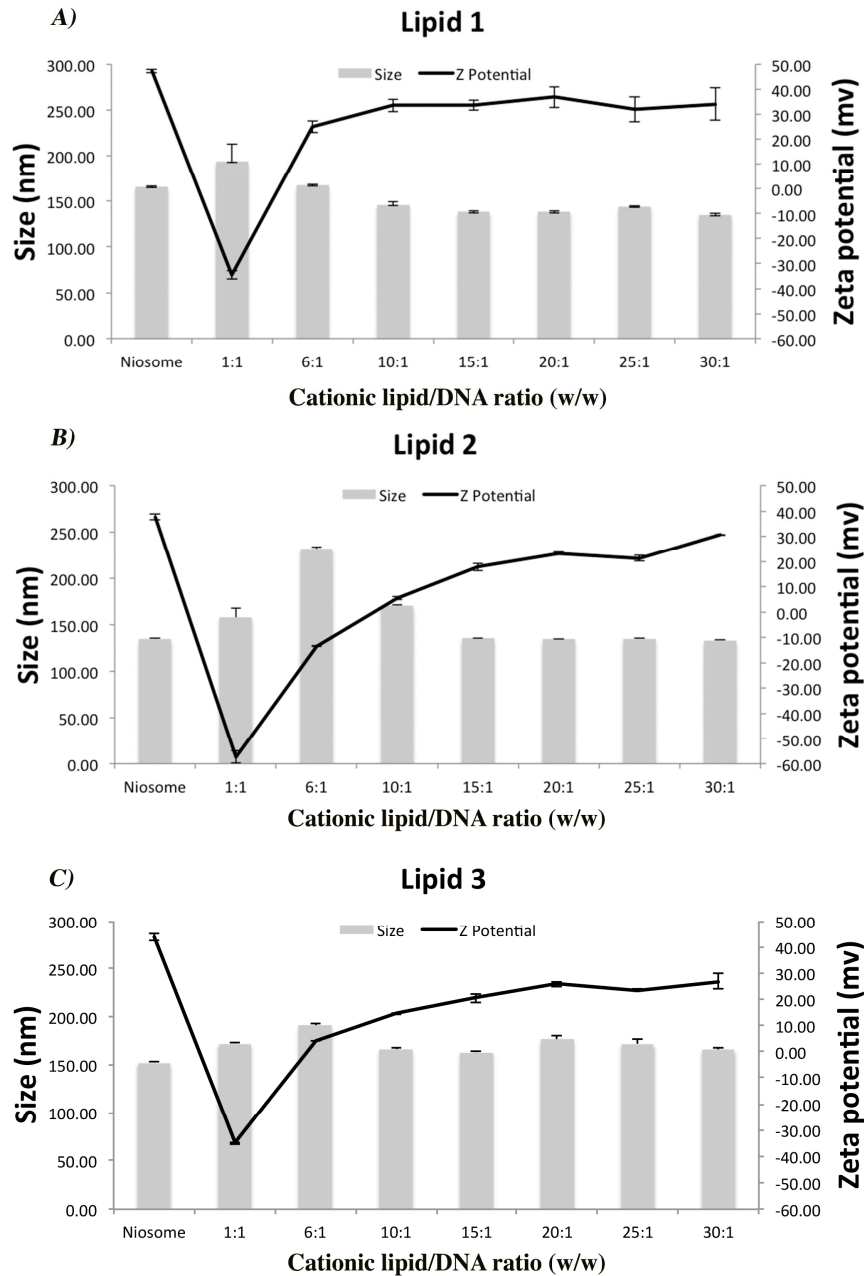
Fig. 4. The influence of the cationic lipid/DNA ratio (w/w) on the particle Z-average (cumulants) size (bars) and zeta potential (lines) of nioplexes based on: (A) lipid **1**, (B) lipid **2** and (C) lipid **3**. Each value represents the mean ± standard deviation of three measurements.

3.4. Characterization of nioplexes in terms of zeta potential and size

Nioplexes formed by the addition of DNA to the niosomes at different cationic lipid/DNA ratios (w/w) were characterized in terms of charge and size (Fig. 4). The results showed a significant decline in zeta potential values (Fig. 4, lines) in the three niosomes formulations when DNA was added at 1/1 cationic lipid/DNA mass ratio (w/w). These changes were observed especially for niosomes based on lipid **2**; zeta potential value decreased from +31 mV to -57 mV (Fig. 4B, line). However, we observed a constant increment of the zeta potential values in all nioplexes formulations with the increment of cationic lipid/DNA

proportion. The maximum positive zeta potential values were observed at 30/1 cationic lipid/DNA ratio (w/w) (+35 mV, +31 mV and +27 mV for nioplexes based on lipids **1**, **2** and **3**, respectively). Our data showed a clear correlation between the cationic lipid/DNA ratios and the superficial charge of the nioplexes, as previously reported [15]. Hence, we can establish an appropriate ratio between cationic lipid and DNA (For lipid **1** and **3** at 6/1 ratio and for lipid **2** at 10/1 ratio (w/w)) to reach positive values, so that nioplexes can interact easily with negatively charged cell membranes.

Concerning about the size of all nioplexes formed with the three niosome formulations (Fig. 4, bars), they did not show relevant differences at mass ratios from 1/1 to 30/1, except lipid **2** at ratio 6/1 (230 nm). Size of the nioplexes can depend on a fragile balance between the ability of cationic lipids to condense the DNA, which can reduce the particle size, and the space demanded by the lipid [7]. Thus, we can explain the slight variation of the size from the lowest to the highest ratio. In general, most of the nioplexes showed a final size below 200 nm, which is a suitable size to be internalized by the cells [30].

3.5. Agarose gel electrophoresis studies of nioplexes

In order to analyze the electrostatic interactions between the niosomes based on the cationic lipids **1**, **2** and **3** and the DNA, we performed an agarose gel electrophoresis assay. Moreover, to study the DNA release, we added SDS to the formulations to simulate an ideal gene delivery condition, where all the cargo is released in the media. We also studied the capacity of niosomes to protect DNA against enzymatic digestion. Based on zeta potential and size data, we selected 6/1, 10/1, 20/1 and 30/1 cationic lipid/DNA ratios (w/w) to perform the agarose gel electrophoresis studies since at cationic lipid/DNA ratios below 6/1, the zeta potential values were negative. The agarose gel electrophoresis assays are shown in Fig. 5, where SC bands show the most bioactive DNA form and OC bands represent structural change of DNA of a less active form [31]. Nioplexes were analyzed in terms of condensation, release and protection of DNA.

First, regarding nioplexes based on cationic lipid **1** (Fig. 5A), the results showed deficient condensation of DNA (lanes 4, 7, 10 and 13), as SC bands were shown in the agarose gel. Moreover, DNAwas easily released from the niosomes at mass ratios 6/1 and 10/1 (lanes 5 and 8) upon the addition of the tensoactive agent SDS, as a possible consequence of poor condensation. We also found that at mass ratios 20/1 and 30/1 there was a weak release of DNA, as white lines were observed at the top of the wells (lanes 11 and 14). This effect was probably due to high zeta potential values (around + 32 mV) obtained at those ratios. In addition, protection of DNA can be observed at all mass ratios. The SC bands in lanes 6, 9, 12 and 15 showed that nioplexes protected the DNA from enzymatic digestion.

Second, regarding nioplexes based on the cationic lipid **2** (Fig. 5B), all ratios were able to condensate the DNA (lanes 4, 7, 10 and 13). The presence of several amino groups in this lipid may be the cause of this level of condensation. On the other hand, the release of DNA at all mass ratios was difficult (lanes 5, 8, 11 and 14), even at lower ratios. Concerning about DNA protection from DNase, we observed reasonable protection at all ratios. Intense OC bands can be observed especially at ratios 6/1, 10/1 and 20/1, which correspond to lanes 6, 9 and 12, as consequence of conformational change of DNA to open circular form due to DNase intervention.

Finally, nioplexes based on the cationic lipid 3 (Fig. 5C) indicated that high DNA condensation was only observed with nioplexes at 30/1 cationic lipid/DNA ratio (w/w) (lane 13), probably due to the high zeta potential values obtained at this ratio (þ27 mV). Moreover, niosomes based on cationic lipid 3 were able to release the DNA especially at low ratios (6/1, lane 5 and 10/1, lane 8). Concerning about protection against enzymatic digestion, nioplexes showed that DNA was properly protected in all cases (lanes 6, 9, 12 and 15).

To summarize, data obtained from agarose gel electrophoresis studies, suggested that nioplexes based on the three cationic lipids, at low ratios (6/1) were less efficient to

condensate, release and protect the DNA against enzymatic digestion. Thus, these outcomes indicated that nioplexes based on lipid 1, 2 and 3 at ratios (w/w) 10/ 1, 20/1 and 30/1 were more suitable to succeed in the transfection experiments.
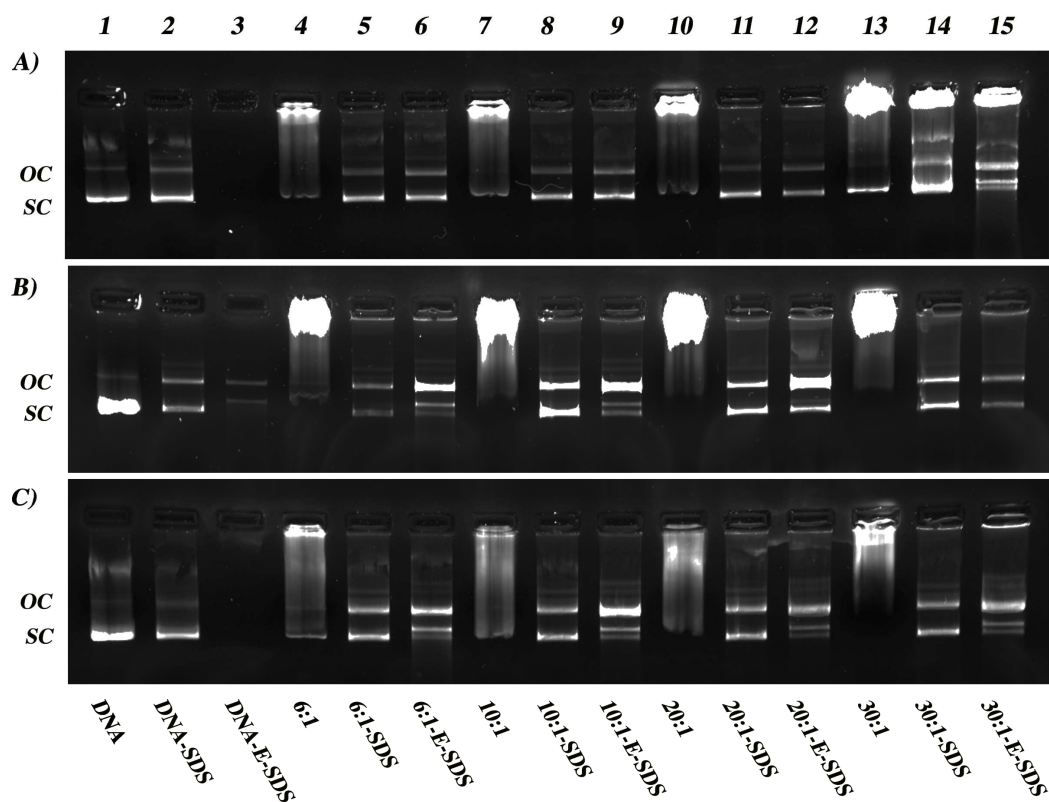

Fig. 5. Binding, protection, and SDS-induced release of DNA from nioplexes at different lipid/DNA (w/w) ratios visualized by agarose electrophoresis. OC: open circular form, SC: supercoiled form. Lanes 1-3 correspond to free DNA; lanes 4-6, cationic lipid/DNA ratio 6/1; lanes 7-9, cationic lipid/DNA ratio 10/1; lanes 10-12, cationic lipid/DNA ratio 20/1; lanes 13-15, cationic lipid/DNA ratio 30/1. Nioplexes were treated with SDS (lanes 2,5,8,11 and 14) and DNase I + SDS (lanes 3,6,9,12 and 15). A) Nioplexes based on lipid **1**, B) nioplexes based on lipid **2** and C) nioplexes based on lipid **3**.

3.6. In vitro transfection experiments in HEK-293, ARPE-19 and PECC cells

We carried out further in vitro assays to analyze transfection efficiencies and toxicity of nioplexes in the following cells: HEK-293 cells, as general cell model, ARPE-19 cells, as retinal cell model for possible in vivo applications in retina, and PECC cells, as neurons and glial model cells for the potential use of nioplexes in the brain (Fig. 6A).

The data obtained from the nioplexes based on the cationic lipid 1 showed that the highest percentage of transfection efficiencies were obtained in HEK-293 cells (around 21%) (Fig. 6A white bars) at mass ratios 20/1 and 30/1. Additionally, suitable transfection results were also observed for ARPE-19 cells, where the highest transfection values were around 18% at 20/1 mass ratio (Fig. 6A gray bars). It must be highlighted that previous work carried out with serinol-based cationic lipids modified with the same lipid tail showed null transfection efficiency in cell culture [15]. These findings suggest that small structural changes in the lipid (serinol by glycerol building block) are enough to influence dramatically on transfections efficiencies. On the other hand, transfections in PECC cells were around 3% for all mass ratios, which was the lowest percent observed within the three types of cells (Fig. 6A black bars). For

nioplexes based on lipid **2**, high percentage of transfected cells were observed again (13%) in HEK-293 cells at ratio 20/1 (w/w) (Fig. 6A white bars). However, low transfection efficiencies were registered in ARPE-19 and PECC cells at all cationic lipid/DNA mass ratios (Fig. 6A gray and black bars, respectively). Similar results also were observed in previous data reported [15] where the cationic lipid formed by longer polyamine chains and more amino nitrogen atoms did not precisely enhanced cell transfection in HEK-293 and ARPE-19 cells. These outcomes are probably due to self-folded conformation that disfavor effective interaction with DNA. It also must be emphasized that presence of more than one carbonyl group in the polar head-group seems to be also an impediment for efficient cell transfections [32,33]. Regarding nioplexes based on lipid **3**, transfections around 20% were obtained in HEK-293 cells at 30/1 mass ratio and lower transfections at 10/1 mass ratio (Fig. 6A white bars). Percentage of transfected cell levels in ARPE-19 cells also showed promising results (19%) at 30/1 mass ratio; similar to the data observed in HEK-293 cells. However, decrease in transfection efficiencies was observed at lower mass ratios (Fig. 6A gray bars). Furthermore, interesting data were obtained in PECC cells, especially at 30/1 mass ratio, where transfection was around 5% (Fig. 6A black bars). For further details regarding confocal microscopy images from transfected cerebral cortical cells, see Supplementary Data, Fig. S1. Cultured neurons are among the most difficult cells to be transfected due to their sensitivity to microenvironmental changes and they tend to die soon after transfection. Typical transfection efficiencies in this kind of cells are around 5% [34]. Interestingly, relevant transfection data in HEK- 293, ARPE-19 and MSC-D1 cells were also observed with a similar cationic lipid that has the same molecular formula, but different structural conformation [15]. In addition, this structural relationship between lipids and transfection has been previously reported by different authors [32,33,35], which have described that slight lipid structure modifications can provoke cell transfection variations.

Cell toxicity is another important issue that has to be addressed for the development of any novel drug delivery system including any desired cationic lipid for its use as non-viral vector. Therefore, we studied the cell viability with our formulations (Fig. 6B). The results indicated that only HEK-293 cells showed high viabilities with nioplexes prepared with lipid **1** (84%, 76% and 70% at 10/1, 20/ 1 and 30/1 mass ratios, respectively). On the other hand, the most toxic effect was observed with the lipid **2** (31% of viability) at 30/1 mass ratio (Fig. 6B white bars). Better toleration in ARPE-19 and PECC cells (Fig. 6B gray and black bars, respectively)was found with nioplexes at all studied ratios (100% of viability) (Fig. 6B gray and black bars). It must be stressed that toxicity effect is, generally, a cell dependent process where every cell type shows different toleration levels [36]. Furthermore, the structure design of the cationic lipids also influences on the cell viability, such as small changes on the polar head-groups that can induce different levels of cytotoxicity [15,37]. It is worth mentioning that cationic lipids containing one or three hydrocarbonated alkyl chains tend to be more toxic and show poor transfection efficiencies [11].

In order to describe more precisely the transfection efficiencies of our formulations, we analyzed the MFI of the EGFP expressed in the transfected cells. Results obtained from the nioplexes based on cationic lipid **1** showed that low MFI were observed in HEK-293 cells (around 30, Fig. 6C white bars) at all tested mass ratios. On the other hand, ARPE-19 and PECC cells showed higher MFI (over 40 and 80, respectively); high MFI in PECC cells were obtained at the three studied mass ratios (10/1, 20/1 and 30/1) (Fig. 6C black bars). Based on the data from nioplexes prepared with the cationic lipid **2**, MFI in HEK-293 cells were around 89 at the different analyzed mass ratios (10/1, 20/1 and 30/1, Fig. 6C white bars). Additionally, expression of EGFP was similar in PECC cells at all analyzed mass ratio (10/1, 20/1 and 30/1, Fig. 6C black bars). MFI results from nioplexes prepared with lipid **3** revealed that HEK-293 cells showed low EGFP expression (MFI around 60) when compared to ARPE-19 and PECC cells. Furthermore, ARPE-19 cells showed the highest MFI (149) at 30/1 mass ratio (Fig. 6C gray bars). The MFI obtained from PECC cells was around 80, which is similar to those observed with the other two cationic lipids (Fig. 6C black bars). Essentially, these results indicated that

nioplexes based on cationic lipid **3** stimulated higher EGFP expression in ARPE-19 transfected cells and suitable expression of EGFP in PECC and HEK-293 transfected cells at 30/1 mass ratio. Likewise, differences in membrane composition among cell lines can also influence cellular uptake and posterior intracellular trafficking processes of vectors [38]. For further MFI information, see histograms in Supplementary Data Fig. S2.
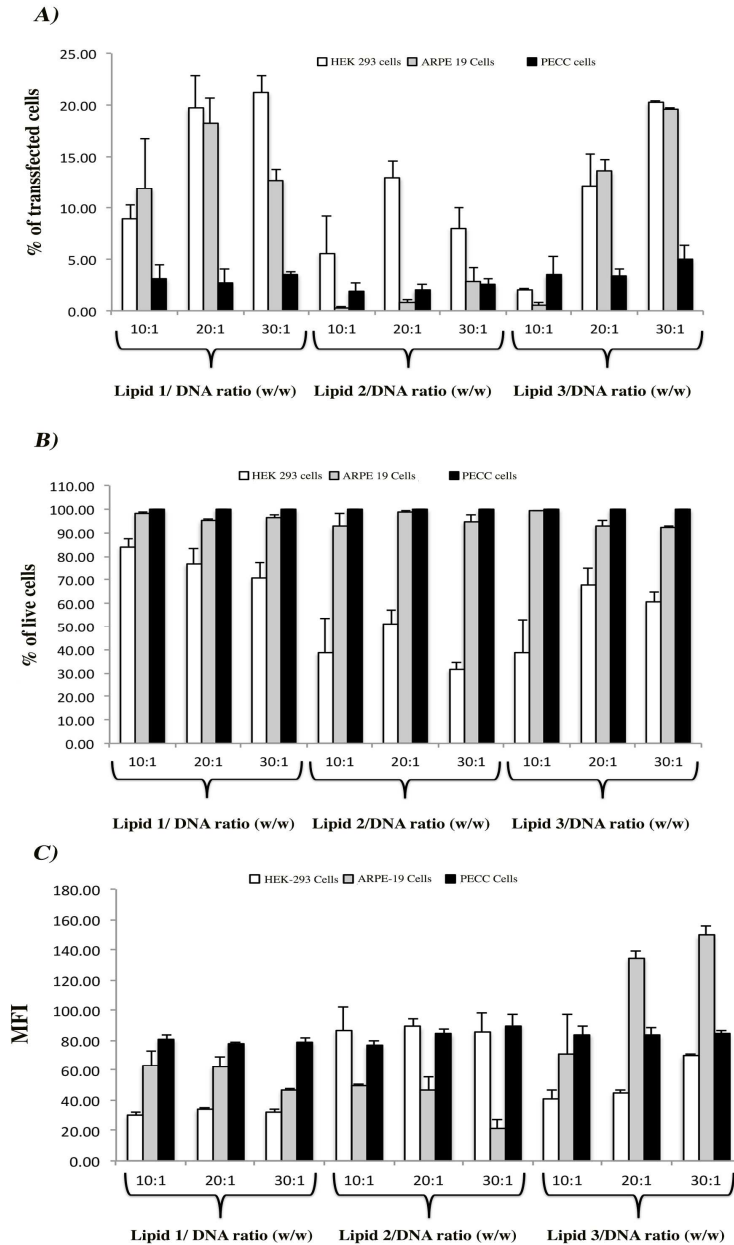

Fig. 6. In vitro transfection experiments of nioplexes based on cationic lipid 1, 2 and 3in HEK-293, ARPE-19 and PECC cells. A) Transfection efficiency at different cationic lipid/DNA ratios (w/w). B) Cell viability at different cationic lipid/DNA ratios (w/w). C) MFI of transfected cells with nioplexes based on cationic lipid 1, 2 and 3 in HEK-293, ARPE-19 and PECC cells at different cationic lipid/DNA ratios (w/w).

Taking into account these data (Fig. 6), nioplexes based on cationic lipid **1** and **3** showed better percentages of transfection in ARPE-19 and PECC cells. These results also indicate that polar headgroups of the cationic lipids play a fundamental role in transfection

efficiencies. In addition, cell toxicity assay showed a cell dependent toxicity effect rather than a polar head-group effect, where major toxicity effect was observed in HEK-293 cells. For MFI assay, the most relevant data were obtained from cationic lipid **3**, which in general expressed high levels of EGFP in cells. Thus, we decided to use niosomes based on lipid 3 as the most appropriate system for further in vivo experiments.

Differences observed among the three cationic lipids on transfection efficiency could be explained, in part, by slight changes on their particle size and superficial charge that affect to their capacity to condense, protect and release the DNA against enzymatic digestion. Additionally, other physicochemical parameters related with the chemical structure of the polar-head group such as the balance between the cross-sectional area of the polar-head group (small end) and the hydrophobic domain (large end), or the pKa value should also be considered. The greater the imbalance between both the polar-head group and the hydrophobic domain, the more unstable the resulting lipid assembly and therefore, the greater the probability to undergo fusion with anionic vesicles [37]. Consequently, this hypothesis could explain the low percentages of transfected cells observed in nioplexes prepared with lipid **2**. Regarding the pKa value, it has been suggested an optimal value slightly inferior to 7 in order to maintain a neutral surface charge density at pH 7.4 [39]. Previous results by our group have shown that dimethylaminoethyl pendent group provides pKa values that could fall in the optimal range for transfection (from 6.2 to 6.7) [15]. Consequently, cationic lipid **3** positive charge density should increase in the acidic environment of the endosome leading to a membrane-destabilizing process by forming ion pairs between the lipid **3** and phospholipids in the endosomal membrane. This process might promote a lamellar to hexagonal transition in the lipid **3** which might disrupt the membrane and destabilize bilayers. Additionally, the presence of squalene in our formulation would facilitate this kind of transition [7]. The combination of these two effects would make this transfection process more efficient.

3.7. In vivo studies

We carried out in vivo studies to evaluate EGFP expression in the rat retina after both subretinal (Fig. 7) and intravitreal (Fig. 8) injections. Both administration routes are clinically viable options to deliver genetic material to the retina [40]. While classically, the effect of subretinal injection is localized around the injection site, intravitreal injections can carry the delivered material to a larger retinal surface [41]. In our results, subretinal injection of nioplexes based on cationic lipid 3 at 30/1 mass ratio resulted in substantial protein expression mainly observed in photoreceptors and in some nuclei in the outer nuclear layer (Fig. 7). Transfection at this level could be of great interest, since most of the inherited retinal diseases such as Stargat Disease, Retinitis Pigmentosa, Age-related Macular Degeneration or Leber Congenital Amaurosis are classically associated to mutations in genes expressed in photoreceptors and outer nuclear layers of the retina [17]. Therefore, subretinal administration of nioplexes based on cationic lipid 3 could be appropriate to treat aforementioned retinal inherited diseases. However, subretinal administration is frequently associated with high risk of retinal detachment or severe lesions in the retina, which often dissuade its clinical application. In any case, some promising results have been obtained in clinical trials after subretinal injection to treat many inherited retinal diseases such as Leber Congenital Amaurosis Type 2 [42].

By contrast, intravitreal injection is a safer technique in ophthalmology and is more widely used in the clinical practice. We found a good and uniformly distributed EGFP expression mainly in the ganglion cell layer and inner layers of the retina 3 days after intravitreal injection of nioplexes based on cationic lipid **3** at 30/1 mass ratio (Fig. 8), which suggests that nioplexes did not aggregate with the negatively charged components of the vitreous humor such as glycosamineglycanes and diffused through the inner layer of the retina, enhanced probably, by the ability of the PEG chains of the polysorbate 80 structure to prevent aggregations due to interaction with fibrilar structures in the vitreous [43,44]. Transfection at

the inner layers of the retina could be of great interest to treat some genetic pathologies of the retina such us glaucoma [45] a progressive optic neuropathy that affect to retinal ganglion cells. Interestingly, we detected some protein expression in the retinal pigmented epithelium (Fig. 8E), which clearly represents a great challenge for retinal gene therapy in order to avoid subretinal injection to target the outer segments of the photoreceptors and the pigmented epithelium cells without causing harm to the sensitive neural tissue [2].
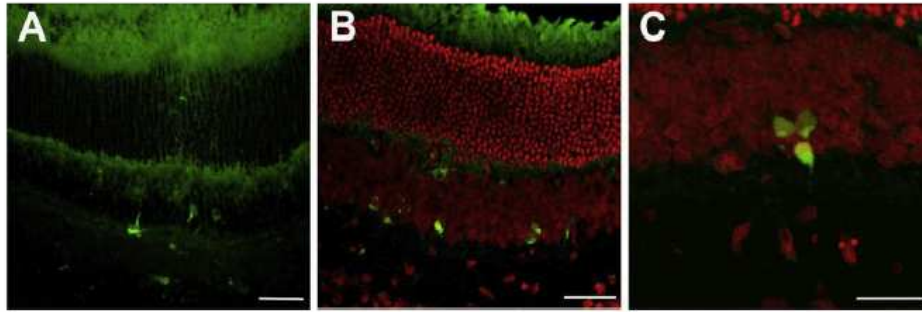
Fig. 7. EGFP gene expression in retina 3 days after subretinal injection of nioplexes based on lipid 3 at mass ratio 30/1 cationic lipid/DNA. A), B) Retinal sections showing EGFP expression mainly in photoreceptors and in some nuclei in the outer nuclear layer (ONL). C) Detail of three EGFP$^+$ cell nuclei located in the ONL. Cell nuclei were counterstained with Hoechst 33342 (red color) in B and C. Scale bars A, B = 40 mm; C = 25 mm. (For interpretation of the references to color in this figure legend, the reader is referred to the web version of this article.)

Additionally, we decided to evaluate the capacity of nioplexes based on lipid **3** at 30/1 ratio to transfect the rat cerebral cortex (Fig. 9). We identified by immunochemistry analysis NeuNþ (red channel), NeuN$^-$ cells and GFP$^+$ (green channel). The NeuN$^+$ corresponded to neurons, NeuN$^-$ to non-neuronal cells, such as glial and endothelia population cells and GFP$^+$ corresponded to cells expressing EGFP. Based on the analysis, we were able to identify neurons and non-neuronal cells that expressed EGFP in the area next to the injection site. Thus, on the one hand, Fig. 9A shows NeuN$^+$ cells that corresponded to neurons expressing high levels of GFP in the cells bodies and in their dendritic trees (white arrows). On the other hand, Fig. 9B shows NeuN$^-$ cells with glial morphology that expressed high levels of GFP throughout the dendritic processes (yellow arrows). Briefly, it seems that there is a cell dependent effect for the nioplexes internalization and transfection process. Favorably, nioplexe injections did not affect the behavior of the animals and no loss of weight was detected during the 3 days of the experimental period. Even though delivering genetic material to the nervous system cells by non-viral vectors remains as a challenge, our nioplexes were able to transfect glial cells and identified neurons in the primary visual cortex in vivo. In this preliminary study, we determined that our nioplexes were able to transfect more glial cells than neurons. These results suggest that cell division of glial cells and the CMV promoter of pCMS-EGFP plasmid could be involved in the transfection process [46]. Therefore, the use of our nioplexes combined with plasmids holding different promoters might allow targeting different cell populations of the nervous system and enhance cell transfection in order to treat different genetic population deficits. Overall, our results open a safe alternative to the treatment of neurodegenerative diseases, such as Parkinson's disease. Despite the current advances to treat these types of diseases, neurodegenerative diseases still do not have effective pharmacotherapy treatments. Therefore, further research is required before these findings can reach the clinic.
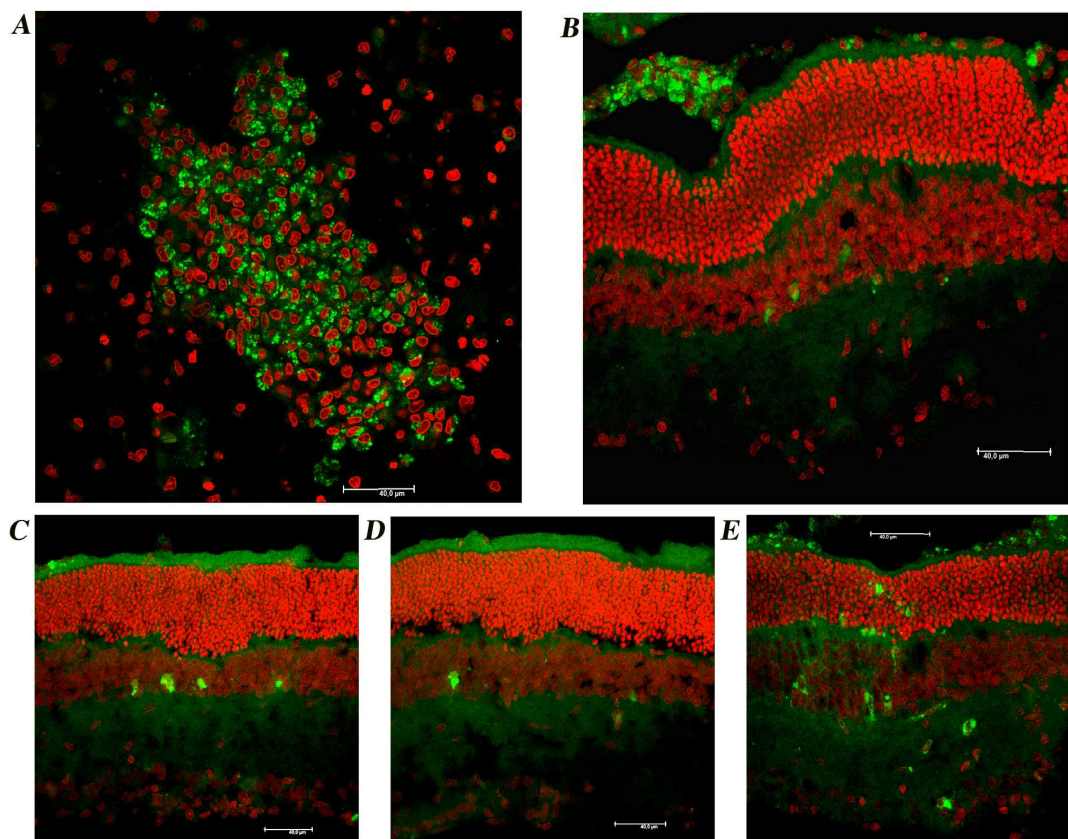
Fig. 8. EGFP gene expression in retina 3 days after intravitreal injection of nioplexes based on lipid 3 at mass ratio 30/1 cationic lipid/DNA. A) Wholemount preparation showing EGFPþ cell bodies located in the ganglion cell layer (GCL). B), C), D) and E) Retinal cross sections. EGFP expression was detected throughout the whole retina although mainly in inner layers. Cell nuclei were counterstained with Hoechst 33342 (red color). Scale bar ¼ 40 mm. (For interpretation of the references to color in this figure legend, the reader is referred to the web version of this article.)

4. Conclusion

In the present study, we designed niosomes prepared from squalene, as helper lipid, polysorbate 80, as non-ionic surfactant and three synthetized cationic lipids, which differed only in the polar head-group, to evaluate their transfection efficiency in retina and brain. Our results showed that the chemical composition of the cationic lipid head-groups clearly affects the physicochemical parameters of the niosomes and modifies the levels of transfection efficiencies of the nioplexes. We observed that niosomes based on cationic lipids with a dimethyl amino (lipid **3**) and amino (lipid **1**) head-groups showed remarkable percentages of transfection capacity when they were compared to their counterpart triglycine head-group (lipid **2**). Regarding MFI, nioplexes based on the cationic lipid **3** showed higher protein expression in the transfected cells when they were compared to lipid **1**. Moreover, in vitro results at different cationic lipid/DNA ratios (w/w) suggested that not only structural changes in the polar head-groups of these cationic lipids were involved in the success of these vectors, but also cationic lipid/ DNA ratios were deeply involved in the interaction with the cells and their transfection efficiencies. In vivo results showed that after subretinal, intravitreal and brain injections, nioplexes transfected successfully the cells in rat retina and brain. Although this preliminary study highlights the flattering properties of nioplexes based on lipid **3** to deliver genetic material to the retina and brain, additional work, such as the long term

evaluation of the transgene expression should also be investigated in order to translate preclinical results in animals to clinical trials.
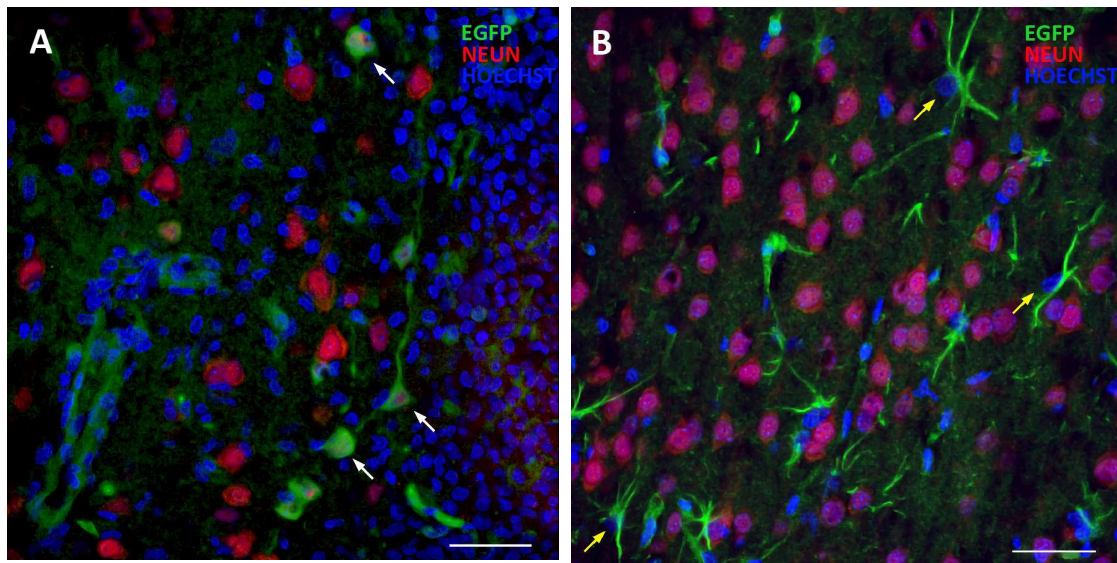

Fig. 9. In vivo gene expression of EGFP 3 days after the administration of nioplexes based on lipid 3 at 30/1 mass ratio cationic lipid/DNA. A and B panels show triple labeling; nuclei are shown in blue (Hoechst), neurons in red (NeuN[+]), and EGFP expressed in cells (GFP[+]) in green. A) Several of the identified neurons (red) that express EGFP (green) in the membrane at their cell bodies and dendritic trees are indicated by white arrows. B) Several of the non-neuron cells (NeuN[-]) with glia morphology that express EGFP (green) through their processes are indicated by yellow arrows. Scale bar = 40 mm. (For interpretation of the references to color in this figure legend, the reader is referred to the web version of this article.)

REFERENCES

[1] H. Yin, R.L. Kanasty, A.A. Eltoukhy, A.J. Vegas, J.R. Dorkin, D.G. Anderson, Nonviral vectors for gene-based therapy, Nat. Rev. Genet. 15 (2014) 541-555.
[2] P. Charbel Issa, R.E. MacLaren, Non-viral retinal gene therapy: a review, Clin. Exp. Ophthalmol. 40 (2012) 39-47.
[3] M. Agirre, J. Zarate, E. Ojeda, G. Puras, L.A. Rojas, R. Alemany, et al., Delivery of an adenovirus vector plasmid by ultrapure oligochitosan based polyplexes, Int. J. Pharm. 479 (2015) 312-319.

[4] M.A. Zarbin, C. Montemagno, J.F. Leary, R. Ritch, Nanomedicine for the treatment of retinal and optic nerve diseases, Curr. Opin. Pharmacol. 13 (2013) 134-148.

[5] P. Arukuusk, L. Parnaste, M. Hallbrink, U. Langel, PepFects and NickFects for the intracellular delivery of nucleic acids, Methods Mol. Biol. 1324 (2015) 303-315.

[6] R. Rajera, K. Nagpal, S.K. Singh, D.N. Mishra, Niosomes: a controlled and novel drug delivery system, Biol. Pharm. Bull. 34 (2011) 945-953.

[7] G. Puras, M. Mashal, J. Zarate, M. Agirre, E. Ojeda, S. Grijalvo, et al., A novel cationic niosome formulation for gene delivery to the retina, J. Control Release 174 (2014) 27e36.

[8] P. Couvreur, "Squalenoylation": a new approach to the design of anticancer and antiviral nanomedicines, Bull. Acad. Natl. Med. 193 (2009) 663-673 discussion 673-4.

[9] H. Chung, T.W. Kim, M. Kwon, I.C. Kwon, S.Y. Jeong, Oil components modulate physical characteristics and function of the natural oil emulsions as drug or gene delivery system, J. Control. Release 71 (2001) 339-350.

[10] F. Liu, J. Yang, L. Huang, D. Liu, New cationic lipid formulations for gene transfer, Pharm. Res. 13 (1996) 1856-1860.

[11] G. Byk, C. Dubertret, V. Escriou, M. Frederic, G. Jaslin, R. Rangara, et al., Synthesis, activity, and structureeactivity relationship studies of novel cationic lipids for DNA transfer, J. Med. Chem. 41 (1998) 229-235.

[12] Y.V. Mahidhar, M. Rajesh, A. Chaudhuri, Spacer-arm modulated gene delivery efficacy of novel cationic glycolipids: design, synthesis, and in vitro transfection biology, J. Med. Chem. 47 (2004) 3938-3948.

[13] P.P. Karmali, A. Chaudhuri, Cationic liposomes as non-viral carriers of gene medicines: resolved issues, open questions, and future promises, Med. Res. Rev. 27 (2007) 696-722.

[14] D. Zhi, S. Zhang, B. Wang, Y. Zhao, B. Yang, S. Yu, Transfection efficiency of cationic lipids with different hydrophobic domains in gene delivery, Bioconjug. Chem. 21 (2010) 563-577.

[15] E. Ojeda, G. Puras, M. Agirre, J. Zarate, S. Grijalvo, R. Pons, et al., Niosomes based on synthetic cationic lipids for gene delivery: the influence of polar head-groups on the transfection efficiency in HEK-293, ARPE-19 and MSC-D1 cells, Org. Biomol. Chem. 13 (2015) 1068-1081.

[16] C. Bloquel, J.L. Bourges, E. Touchard, M. Berdugo, D. BenEzra, F. Behar-Cohen, Non-viral ocular gene therapy: potential ocular therapeutic avenues, Adv. Drug Deliv. Rev. 58 (2006) 1224-1242.

[17] D.M. Lipinski, M. Thake, R.E. MacLaren, Clinical applications of retinal gene therapy, Prog. Retin. Eye Res. 32 (2013) 22e47.

[18] S. Nagabhushan Kalburgi, N.N. Khan, S.J. Gray, Recent gene therapy advancements for neurological diseases, Discov. Med. 15 (2013) 111-119.

[19] S. Worgall, D. Sondhi, N.R. Hackett, B. Kosofsky, M.V. Kekatpure, N. Neyzi, et al., Treatment of late infantile neuronal ceroid lipofuscinosis by CNS administration of a serotype 2 adeno-associated virus expressing CLN2 cDNA, Hum. Gene Ther. 19 (2008) 463-474.

[20] P. Leone, D. Shera, S.W. McPhee, J.S. Francis, E.H. Kolodny, L.T. Bilaniuk, et al., Long-term follow-up after gene therapy for canavan disease, Sci. Transl. Med. 4 (2012), 165-163.

[21] S. Muramatsu, The current status of gene therapy for Parkinson's disease, Ann. Neurosci. 17 (2010) 92-95.

[22] C. Soto-Sanchez, G. Martinez-Navarrete, L. Humphreys, G. Puras, J. Zarate, J.L. Pedraz, et al., Enduring high-efficiency in vivo transfection of neurons with non-viral magnetoparticles in the rat visual cortex for optogenetic applications, Nanomedicine 11 (2015) 835-843.

[23] G. Puras, J. Zarate, M. Aceves, A. Murua, A.R. Diaz, M. Aviles-Triguero, et al., Low molecular weight oligochitosans for non-viral retinal gene therapy, Eur. J. Pharm. Biopharm. 83 (2) (2012) 131-140.

[24] M. Jayaraman, S.M. Ansell, B.L. Mui, Y.K. Tam, J. Chen, X. Du, et al., Maximizing the potency of siRNA lipid nanoparticles for hepatic gene silencing in vivo, Angew. Chem. Int. Ed. Engl. 51 (2012) 8529-8533.

[25] G. Caracciolo, H. Amenitsch, Cationic liposome/DNA complexes: from structure to interactions with cellular membranes, Eur. Biophys. J. 41 (2012) 815-829.

[26] Z. Rezvani Amin, M. Rahimizadeh, H. Eshghi, A. Dehshahri, M. Ramezani, The effect of cationic charge density change on transfection efficiency of polyethylenimine, Iran. J. Basic Med. Sci. 16 (2013) 150-156.

[27] G. Caracciolo, R. Caminiti, M.A. Digman, E. Gratton, S. Sanchez, Efficient escape from endosomes determines the superior efficiency of multicomponent lipoplexes, J. Phys. Chem. B 113 (2009) 4995-4997.

[28] S.E. Gratton, P.A. Ropp, P.D. Pohlhaus, J.C. Luft, V.J. Madden, M.E. Napier, et al., The effect of particle design on cellular internalization pathways, Proc. Natl. Acad. Sci. U. S. A. 105 (2008) 11613-11618.

[29] B. Heurtault, P. Saulnier, B. Pech, J.E. Proust, J.P. Benoit, Physico-chemical stability of colloidal lipid particles, Biomaterials 24 (2003) 4283-4300.

[30] J. Rejman, V. Oberle, I.S. Zuhorn, D. Hoekstra, Size-dependent internalization of particles via the pathways of clathrin- and caveolae-mediated endocytosis, Biochem. J. 377 (2004) 159-169.

[31] N.C. Stellwagen, E. Stellwagen, Effect of the matrix on DNA electrophoretic mobility, J. Chromatogr. A 1216 (2009) 1917-1929.

[32] K. Takeuchi, M. Ishihara, C. Kawaura, M. Noji, T. Furuno, M. Nakanishi, Effect of zeta potential of cationic liposomes containing cationic cholesterol derivatives on gene transfection, FEBS Lett. 397 (1996) 207-209.

[33] T. Fujiwara, S. Hasegawa, N. Hirashima, M. Nakanishi, T. Ohwada, Gene transfection activities of amphiphilic steroidepolyamine conjugates, Biochimica Biophysica Acta BBA Biomembr. 1468 (2000) 396-402.

[34] D. Karra, R. Dahm, Transfection techniques for neuronal cells, J. Neurosci. 30 (2010) 6171-6177.

[35] O. Paecharoenchai, N. Niyomtham, A. Apirakaramwong, T. Ngawhirunpat, T. Rojanarata, B.E. Yingyongnarongkul, et al., Structure relationship of cationic lipids on gene transfection mediated by cationic liposomes, AAPS PharmSci- Tech 13 (2012) 1302-1308.

[36] S.K. Sohaebuddin, P.T. Thevenot, D. Baker, J.W. Eaton, L. Tang, Nanomaterial cytotoxicity is composition, size, and cell type dependent, Part Fibre Toxicol. 7 (2010), 22-8977-7-22.

[37] B. Martin, M. Sainlos, A. Aissaoui, N. Oudrhiri, M. Hauchecorne, J.P. Vigneron, et al., The design of cationic lipids for gene delivery, Curr. Pharm. Des. 11 (2005) 375-394.

[38] D. Pozzi, C. Marchini, F. Cardarelli, F. Salomone, S. Coppola, M. Montani, et al., Mechanistic evaluation of the transfection barriers involved in lipid-mediated gene delivery: interplay between nanostructure and composition, Biochim. Biophys. Acta 1838 (2014) 957-967.

[39] S.C. Semple, A. Akinc, J. Chen, A.P. Sandhu, B.L. Mui, C.K. Cho, et al., Rational design of cationic lipids for siRNA delivery, Nat. Biotechnol. 28 (2010) 172-176.

[40] S.M. Conley, M.I. Naash, Nanoparticles for retinal gene therapy, Prog. Retin. Eye Res. 29 (2010) 376-397.

[41] P. Dureau, L. Legat, M. Neuner-Jehle, S. Bonnel, S. Pecqueur, M. Abitbol, et al., Quantitative analysis of subretinal injections in the rat, Graefes Arch. Clin. Exp. Ophthalmol. 238 (2000) 608-614.

[42] J. Bennett, M. Ashtari, J. Wellman, K.A. Marshall, L.L. Cyckowski, D.C. Chung, et al., AAV2 gene therapy readministration in three adults with congenital blindness, Sci. Transl. Med. 4 (2012), 120ra15.

[43] G.P. Ochoa, J.Z. Sesma, M.A. Diez, A. Diaz-Tahoces, M. Aviles-Trigeros, S. Grijalvo, et al., A novel formulation based on 2,3-di(tetradecyloxy)propan- 1-amine cationic lipid combined with polysorbate 80 for efficient gene delivery to the retina, Pharm. Res. 31 (2014) 1665-1675.

[44] L. Peeters, N.N. Sanders, K. Braeckmans, K. Boussery, J. Van de Voorde, S.C. De Smedt, et al., Vitreous: a barrier to nonviral ocular gene therapy, Investig. Ophthalmol. Vis. Sci. 46 (2005) 3553-3561.

[45] X. Liu, C.A. Rasmussen, B.T. Gabelt, C.R. Brandt, P.L. Kaufman, Gene therapy targeting glaucoma: where are we? Surv. Ophthalmol. 54 (2009) 472-486.

[46] S. Kugler, E. Kilic, M. Bahr, Human synapsin 1 gene promoter confers highly neuron-specific long-term transgene expression from an adenoviral vector in the adult rat brain depending on the transduced area, Gene Ther. 10 (2003) 337-347.

Scheme S1. Synthesis of glycerol-based cationic lipids (**2**, **4** and **5**; lipid **1**, **2** and **3**, respectively)
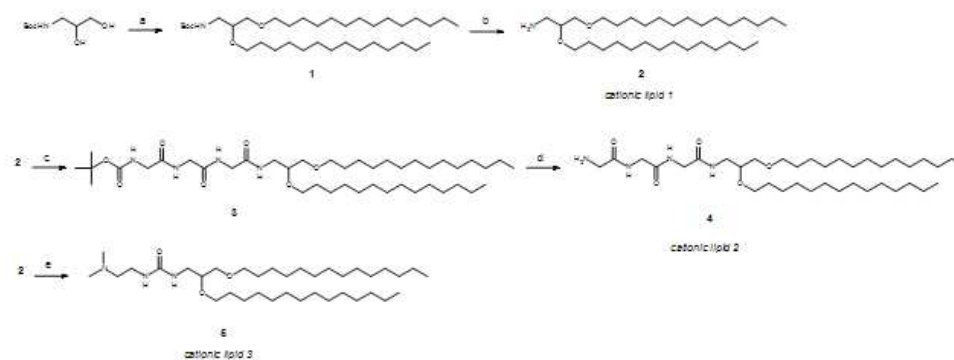
Reagents and Conditions. a and b [7]; c. i. Boc-NH-Gly$_3$-COOH, EDC, NHS, CH$_2$Cl$_2$, overnight, r.t.; ii. 2, DIEA, DMF, overnight, 60 °C; d. i. CH$_2$Cl$_2$:TFA 10%, r.t.; ii. carbonate polymer, MeOH:AcOEt, 1h, r.t.; e. i. p-NO$_2$Ph, THF: CH$_2$Cl$_2$ (1:1), 4h, r.t.; ii. dimethylamine derivative, DMF, overnight, r.t.

tert-butyl-N-[2-[[2-[[2-[2,3-di(tetradecoxy)propylamino]-2-oxo-ethyl]amino]-2-oxo-ethyl]-amino]-2-oxo-ethyl]carbamate (**3**). Yield 70 %, ^{1}H-NMR (400 MHz, CDCl$_3$) δ 7.00 (broad m, NH), 6.93 (broad m, NH), 6.41 (broad m, NH), 4.18 (broad s, NH), 4.00 (d, J = 5.6 Hz, 2H; C$\underline{H}_2$), 3.92 (d, J = 5.5 Hz, 2H; C$\underline{H}_2$), 3.83 (d, J = 5.6 Hz, 2H; C$\underline{H}_2$), 3.48 (m, 9H; 2 C$\underline{H}_2$-O; C$\underline{H}$-N and 2 C$\underline{H}_2$-O), 1.54 (m, 4H; 2 C$\underline{H}_2$), 1.45 (s, 9H; 3 C$\underline{H}_3$-C); 1.28 (m, 44H; alkyl chain), 0.88 (t, J = 6.7 Hz, 6H; 2 C$\underline{H}_3$); ^{13}C-NMR (125 MHz, CDCl$_3$) δ 171.5 (C$\underline{O}$), 170.2 (C$\underline{O}$), 168.9 (C$\underline{O}$), 168.4 (C$\underline{O}$), 80.7 (C-O), 71.8 (C$\underline{H}_2$-O), 71.2 (C$\underline{H}_2$-O), 70.2 (C$\underline{H}_2$-O), 53.4 (C$\underline{H}_2$-N), 42.9 (C$\underline{H}_2$-N), 42.8 (C$\underline{H}_2$-N), 40.9 (C$\underline{H}$-N), 31.9 (C$\underline{H}_3$-C), 29.9, 29.7, 29.6, 29.6, 29.6, 29.4, 29.3, 29.2, 26.1, 26.0, 25.4, 22.6, (alkyl chain) 14.0 (C$\underline{H}_3$-C); ESI-MS for C$_{42}$H$_{82}$N$_4$O$_7$ m/z 755.6183 (calculated) 755.6185 (M+H)$^+$.
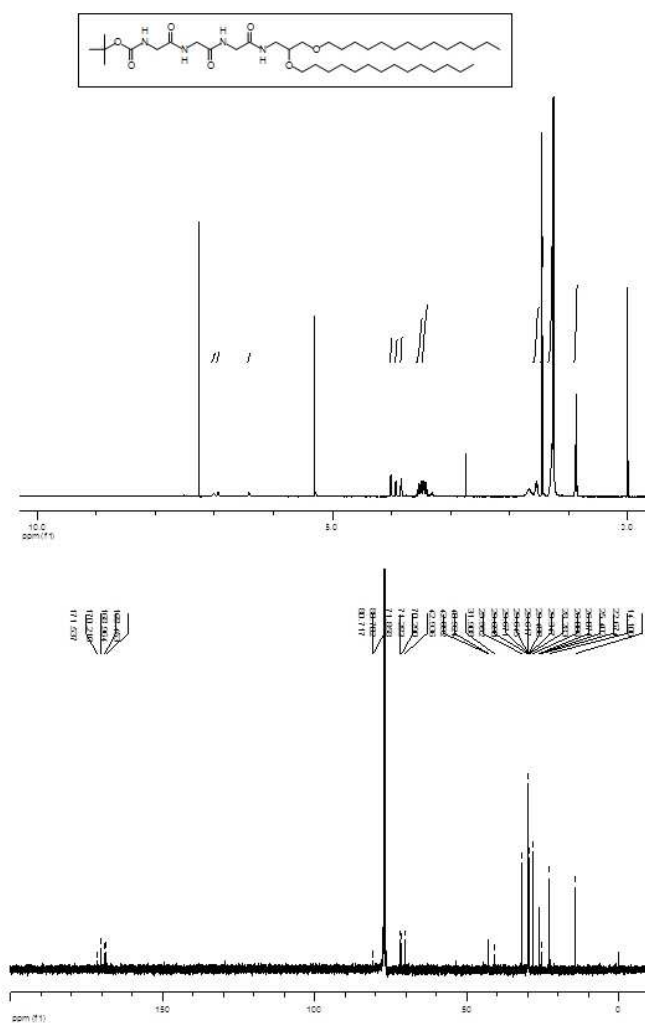
2-[[2-[(2-aminoacetyl)amino]acetyl]amino]-**N**-[2,3-di(tetradecoxy)propyl]acetamide (4, cationic lipid **2**). Yield 87%, ^{1}H-NMR (400 MHz, MeOD:CDCl$_3$) ẟ 3.96 (s, 2H; C$\underline{H}_2$-N), 3.86 (s, 2H; C$\underline{H}_2$-N), 3.71 (s, 2H; C$\underline{H}_2$-N), 3.55 (m, 4H; 2 C$\underline{H}_2$-O), 3.45 (m, 3H; C$\underline{H}_2$O and C$\underline{H}$-NH), 1.55 (m, 2H; C$\underline{H}_2$-C), 1.37 (m, 6H; alkyl chain), 1.27 (m, 38H; alkyl chain), 0.88 (t, J = 7.1 Hz, 6H; 2 C$\underline{H}_3$); ESI-MS for C$_{37}$H$_{74}$N$_4$O$_5$ m/z 655.5659 (calculated) 655.5658 (M+H)$^+$ (found).
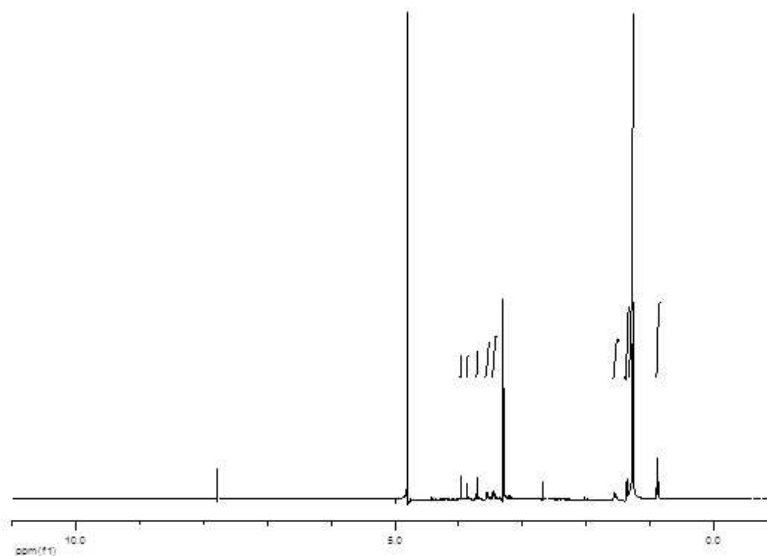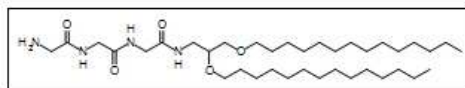
1-(2-dimethylaminoethyl)-3-[2,3-di(tetradecoxy)propyl]urea (5, cationic lipid **3**). Yield 65%; ^{1}H -NMR (400 MHz, CDCl$_3$) ơ 3.44 (m, 6H; 3 C$\underline{H}_2$-O); 3.26 (m, 3H; C$\underline{H}$-N and C$\underline{H}_2$-O); 2.46 (m, 4H; N-C$\underline{H}_2$-C$\underline{H}_2$-N), 2.28 (s, 3H; N-C$\underline{H}_3$), 2.25 (s, 3H; N-C$\underline{H}_3$), 1.55 (m,. 2H; C$\underline{H}_2$-CH$_2$), 1.25 (m, 46H; alkyl chain); 0.88 (t, J = 6.7 Hz; 6H; 2 C$\underline{H}_3$); ^{13}C-NMR (125 MHz, CDCl$_3$) ơ 161.1 ($\underline{C}$O); 158.6 ($\underline{C}$O), 71.7 ($\underline{C}$H$_2$-O), 70.2 ($\underline{C}$H$_2$-O), 58.8 ($\underline{C}$H$_2$-O), 57.5 ($\underline{C}$H-O), 45.0 ($\underline{C}$H$_3$-N), 41.9 (CO-$\underline{C}$H$_2$-N), 37.7 ($\underline{C}$H$_2$-N), 35.2 ($\underline{C}$H$_2$-N), 31.8 ($\underline{C}$H$_2$-N), 30.0, 29.7, 29.6, 29.4, 29.3, 26.1, 22.6 (alkyl chain), 14.0 ($\underline{C}$H$_3$); ESI-MS for C$_{31}$H$_{65}$NO$_2$ m/z 598.5808 (calculated) 598.5806 (M+H)$^+$ (found).
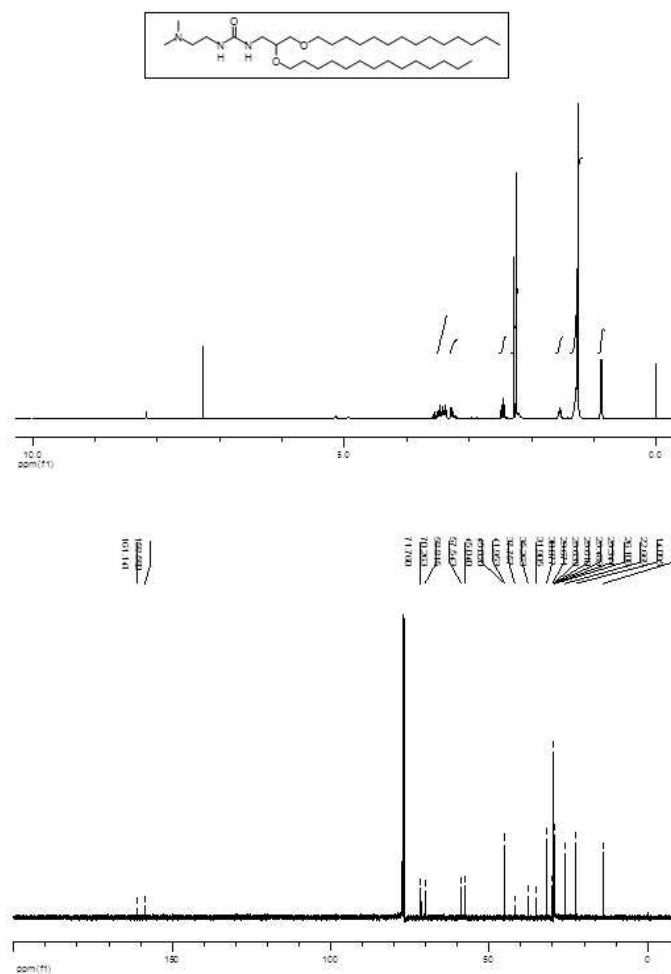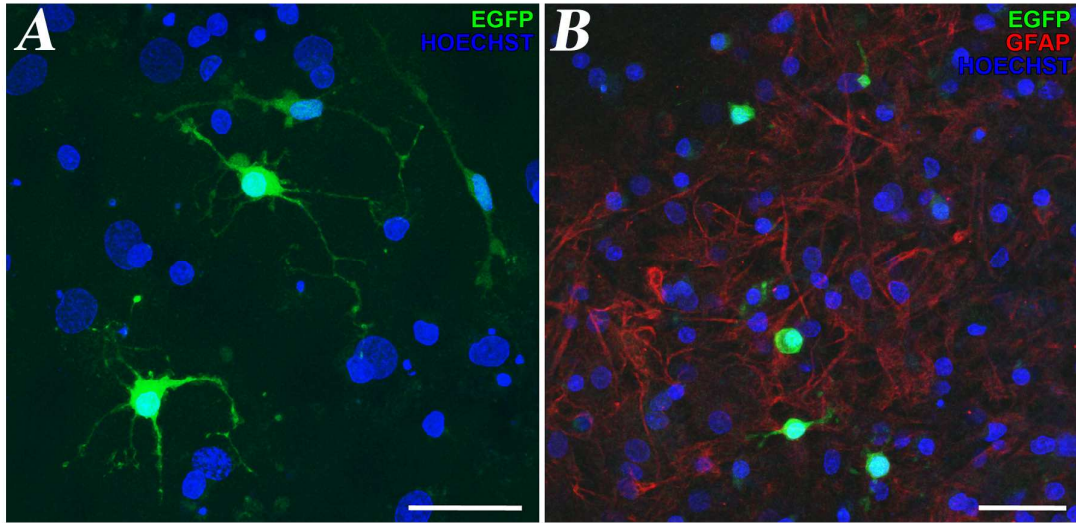
Figure S1. *In vitro* transfection of PECC cells with nioplexes based on cationic lipid **3** at 30/1 cationic lipid/DNA (w/w) ratio. A) Shows direct fluorescence signal of EGFP (green) expression in non-identified cerebral cortical cells. Cell nuclei are marked in blue (Hoechst). B) Shows double labeling with Hoechst (blue) and GFAP (red). Transfected cells show green fluorescence from EGFP expression.
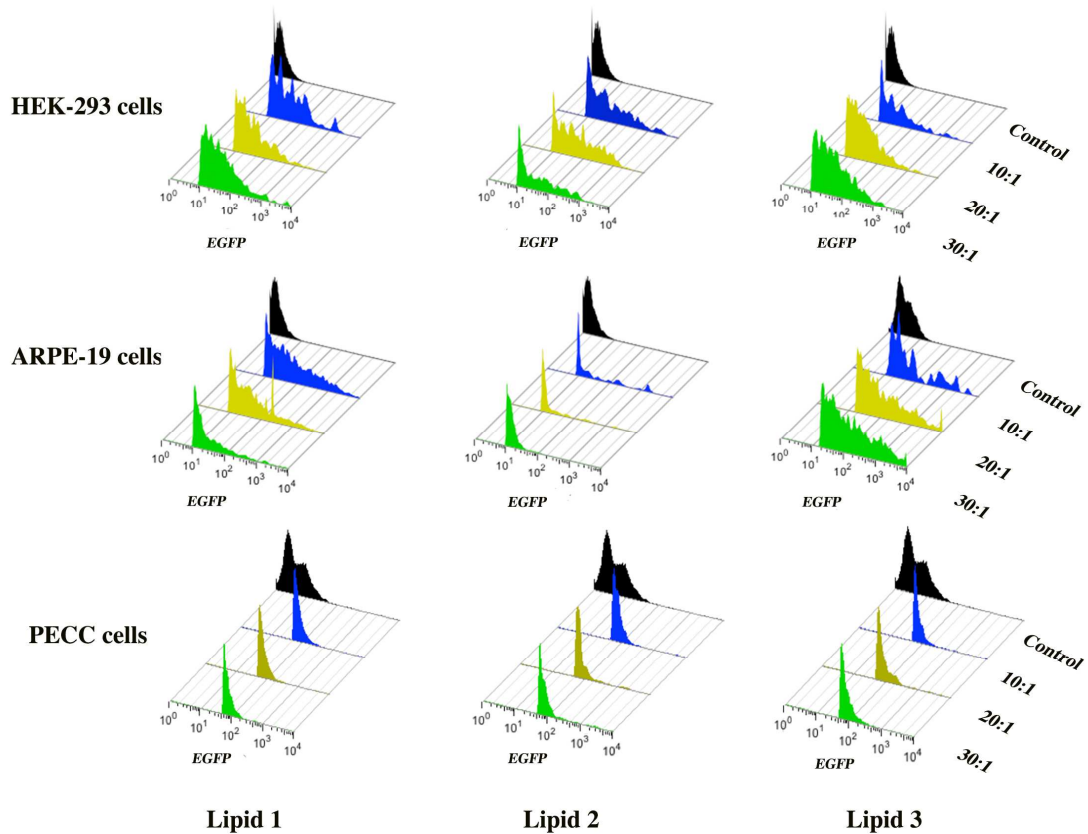
Figure S2. Flow cytometry histograms of transfected cells with nioplexes based on cationic lipid **1**, **2** and **3** in HEK-293, ARPE-19 and PECC cells at different cationic lipid/DNA (w/w) ratios. Color code: Black) control cells, Blue) 10/1 cationic lipid/DNA (w/w) ratio, Yellow) 20/1 cationic lipid/DNA (w/w) ratio and Green) 30/1 cationic lipid/DNA (w/w) ratio. (For interpretation of the references to color in this figure legend, the reader is referred to the web version of the article).